# REPORT DOCUMENTATION PAGE

*Form Approved*
*OMB No. 0704-0188*



| 1. REPORT DATE *(DD-MM-YYYY)* | 2. REPORT TYPE | 3. DATES COVERED *(From - To)* |
|---|---|---|
| 2 June 2003 | Technical Paper | |

**4. TITLE AND SUBTITLE**

**Synthesis and Atomic Oxygen Erosion Testing of Space-Survivability POSS (Polyhedral Oligomeric Silsequioxane) Polyimides**

**5a. CONTRACT NUMBER**

**5b. GRANT NUMBER**

**5c. PROGRAM ELEMENT NUMBER**

**6. AUTHOR(S)**

Rene I. Gonzalez, Sandra J. Tomczak, Timothy K. Minton, Amy Brunsvold, Gar B. Hoflund

**5d. PROJECT NUMBER**
**2303**

**5e. TASK NUMBER**
**M1A3**

**5f. WORK UNIT NUMBER**

**7. PERFORMING ORGANIZATION NAME(S) AND ADDRESS(ES)**

Air Force Research Laboratory (AFMC)
AFRL/PRSM
10 E. Saturn Blvd.
Edwards AFB CA 93524-7680

**8. PERFORMING ORGANIZATION REPORT NUMBER**

AFRL-PR-ED-TP-2003-145

**9. SPONSORING / MONITORING AGENCY NAME(S) AND ADDRESS(ES)**

Air Force Research Laboratory (AFMC)
AFRL/PRS
5 Pollux Drive
Edwards AFB CA 93524-7048

**10. SPONSOR/MONITOR'S ACRONYM(S)**

**11. SPONSOR/MONITOR'S NUMBER(S)**
AFRL-PR-ED-TP-2003-145

**12. DISTRIBUTION / AVAILABILITY STATEMENT**

Approved for public release; distribution unlimited.

**13. SUPPLEMENTARY NOTES**

**14. ABSTRACT**



**15. SUBJECT TERMS**

| 16. SECURITY CLASSIFICATION OF: | | | 17. LIMITATION OF ABSTRACT | 18. NUMBER OF PAGES | 19a. NAME OF RESPONSIBLE PERSON |
|---|---|---|---|---|---|
| | | | | | Sheila Benner |
| a. REPORT | b. ABSTRACT | c. THIS PAGE | A | | 19b. TELEPHONE NUMBER *(include area code)* |
| **Unclassified** | **Unclassified** | **Unclassified** | | | (661) 275-5693 |

FILE

MEMORANDUM FOR PRS (In-House Publication)

FROM: PROI (STINFO)

02 Jun 2003

SUBJECT: Authorization for Release of Technical Information, Control Number: **AFRL-PR-ED-TP-2003-145**
Rene I. Gonzalez and Sandra J. Tomczak, (AFRL/PRSM); Timothy K. Minton and Amy Brunsvold (Montana State Univ); Gar B. Hoflund (Univ of Florida), "Synthesis and Atomic Oxygen Erosion Testing of Space-Survivable POSS (Polyhedral Oligomeric Silsesquioxane) Polyimides"

# SYNTHESIS AND ATOMIC OXYGEN EROSION TESTING OF SPACE-SURVIVABLE POSS (POLYHEDRAL OLIGOMERIC SILSESQUIOXANE) POLYIMIDES

**Rene I. Gonzalez[1], Sandra J. Tomczak[1], Timothy K. Minton[2], Amy L. Brunsvold[2], Gar B. Hoflund[3]**

*[1] AFRL/PRSM, Materials Applications Branch, Air Force Research Laboratory, 10 E. Saturn Blvd, Bldg. 8451, Edwards AFB, CA 93524, USA, rene.gonzalez@edwards.af.mil, sandra.tomczak@edwards.af.mil*

*[2] Department of Chemistry and Biochemistry, Montana State University, 108 Gaines Hall, Bozeman, MT 59717, USA tminton@montana.edu*

*[3] Department of Chemical Engineering, University of Florida, Gainesville, FL 32611, USA*

## ABSTRACT

This paper presents several characterization studies of the surfaces of newly synthesized POSS-containing polyimides before and after exposure to atomic oxygen (AO). AO exposure testing was conducted independently at the University of Florida and Montana State University revealing comparable data. The exposed surfaces were characterized using X-ray photoelectron spectroscopy, and atomic oxygen erosion rates were calculated using stylus surface profilometry. The data indicate that AO induced erosion of polyimides containing POSS is drastically reduced as a result of a passivating silica layer is formed on the surface of the polymer.

## 1. INTRODUCTION

Polyimides such as Kapton, are used extensively on spacecraft primarily as flexible substrates for lightweight, high-power solar arrays because of their inherent strength, temperature stability, excellent insulation properties, UV stability and IR transparency. They are also used in conjunction with Teflon FEP as the outer layer of multi-layer thermal control insulation because of their superior optical properties, including low solar absorptance and high thermal reflectance. In these multilayer insulations a metalized layer is typically applied to the backside in order to reflect incident sunlight. In addition, polyimides are the predominant materials used to build space inflatable structures.

However, over the last twenty years, it has been well established through space-based experiments and ground simulations that polymeric materials and films, undergo severe degradation as a result of the aggressive environment encountered in low Earth orbits (LEO). In this high vacuum environment, materials are subjected to the full spectrum of solar radiation and must endure constant thermal cycling and bombardment by low and high-energy charged particles as well as high incident fluxes of AO. These harsh conditions combined with the need for lighter weight and lower cost man-made orbiting bodies necessitates the design of multi-functional, space-survivable materials.

Hybrid inorganic/organic polymers have the potential to meet the requirements of space-survivable materials by bridging the gap between ceramics and plastics, resulting in the prevention of AO and radiation damage that has hampered the widespread application of organic polymers in space. The Polymer Working Group at the Air Force Research Laboratory at Edwards AFB has incorporated inorganic POSS (Polyhedral Oligomeric Silsesquioxane) frameworks into traditional polymer systems resulting in hybrid POSS-polymers with dramatic property enhancements [1-3]. POSS frameworks (Fig. 1) are comprised of a three dimensional inorganic cage structure with a 2:3 Si:O ratio, surrounded by tailorable organic groups [4-6].

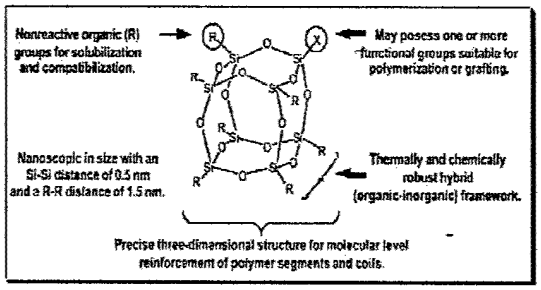


Fig. 1. Anatomy of a POSS nanostructure

They are functionalized monomers that can be copolymerized, grafted and blended into traditional polymer systems [7]. The anatomy of a POSS molecule shown in Fig. 1 is defined by the following features: (1) Single molecules with dimensions ranging in size from 0.7 nm to 3 nm with an average of 1.5 nm rendering them approximately two orders of magnitude smaller than conventional inorganic fillers (quartz talc ~ 100 μm, fumed Si ~100 nm, colloidal $SiO_2$ ~ 10 nm). (2) A thermally and chemically robust inorganic framework with well defined three-dimensional polyhedral geometries. (3) One or more functional groups which enable grafting and copolymeriztion. (4) Nonreactive R groups (cyclopentyl, cyclohexyl, phenyl, isobutyl, methyl) which aid in the compatibilization with the polymer matrix [3,7]. Addition of these POSS nanostructured frameworks into polymers results in increased use and

decomposition temperatures, improved mechanical properties, and oxidation resistance.

Our previous research has shown that chemical manipulation of the unreactive organic groups surrounding the POSS cage [3,7] enables dispersion of POSS nanostructures throughout the polymer matrix at high POSS loadings via blending and copolymerization techniques [1,2,7]. We have also shown that polymers containing POSS rapidly form a ceramic-like, passivating and self-healing silica layer when exposed to high incident fluxes of AO [8-10]. We believe that this self-healing nature is a direct result of POSS compatibility and dispersion throughout the polymer matrix. If the glassy silica layer erodes or suffers a microdefect, it would quickly reform due to the uniform POSS dispersion.

This paper presents a characterization study of the surfaces of newly synthesized POSS-containing polyimides before and after exposure to AO. Atomic oxygen exposure testing was conducted independently at the University of Florida and Montana Sate University revealing comparable data. The exposed surfaces were characterized using X-ray photoelectron spectroscopy, and atomic oxygen erosion rates were calculated using stylus surface profilometry. Changes in the surface topography were measured using atomic force microscopy.

## 2. RESULTS AND DISCUSSION

### 2.1 Synthesis of POSS Polyimide Copolymers

A POSS framework **1** with two anilino pendant groups was provided by Prof. Frank Feher and prepared as described in [11]. Using this monomer, various POSS-polyimide random copolymers were synthesized as shown in Fig. 2 with POSS loadings corresponding to 0, 5, 10 and 20 wt%.

### 2.2 Thermo-mechanical Properties of POSS-Polyimides

The linear viscoelastic properties of polyimides with differing amounts of POSS incorporation were determined using a dynamical mechanical analyzer in tensile mode over a wide range of temperatures. Fig. 3 presents a comparison of storage modulus, E'(T), as a function of temperature for polyimides with 0 wt%, 5 wt%, and 10 wt% POSS segments, respectively. All polymers exhibited a mechanical relaxation transition at temperature near 400 °C indicating the onset of large scale thermally induced motions. It is well known that this type of polyimide, Kapton, does not flow at elevated temperature. This was confirmed by the change in the magnitude of E'(T) at the transition temperature, i.e., from around 1 GPa to 100 MPa. Normal (flexible) polymers would have dropped down to about 1 MPa. As shown in Fig. 3, at temperatures below this relaxation, the magnitude of E'(T) was not significantly affected by the addition of POSS segments in the polymer chain. However, at temperatures above this relaxation, the magnitude of E'(T) increases as the amount of POSS segments in the polymer chain increases.

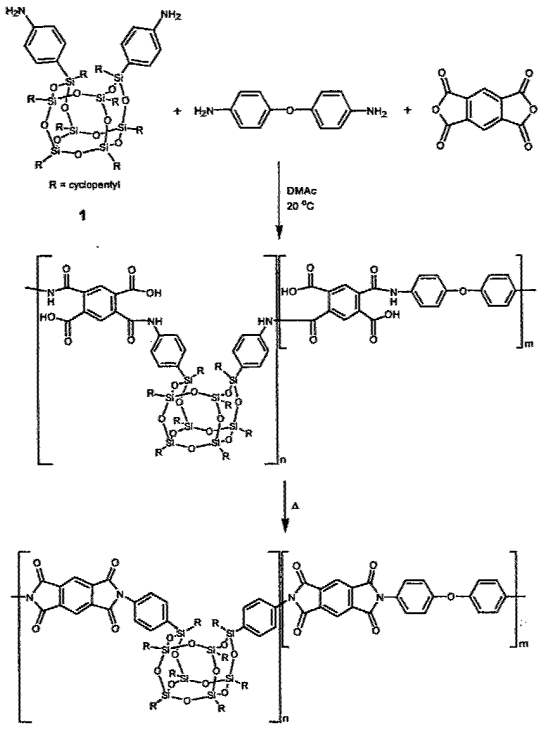


Fig. 2. Synthesis of POSS-Polyimides

The corresponding value of the plateau moduli depends on the amount of POSS incorporation in the polymer. The appearance of these plateaus at temperatures above the mechanical relaxation transition indicate a very strong POSS-POSS interaction where the modulus of polymer was not affected by the change in temperature. These observations suggest that POSS-POSS interactions reduce the motion of the polymer chains and add mechanical strength to these polymer systems above the glass transition in a manner that could be analogous to entanglements.

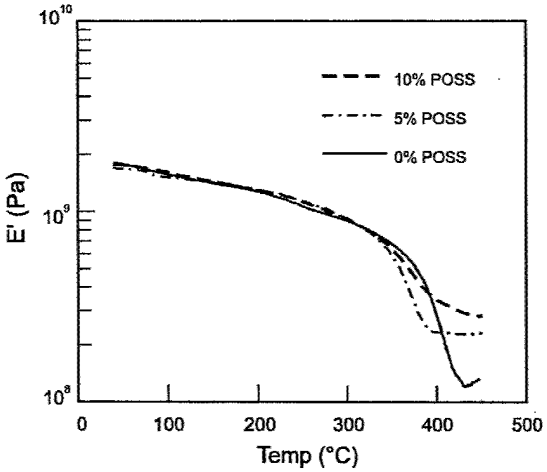


Fig. 3 Plot of storage modulus E'(T) vs. temperature for Kapton and POSS-Kapton polymers

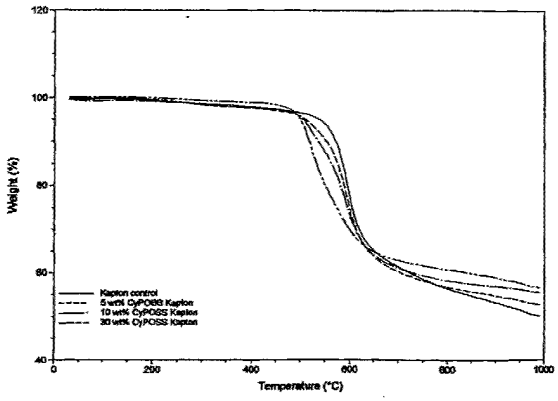


Fig. 4. TGA for Kapton and POSS-Kapton polyimides under $N_2$, 10 °C/min heat ramp

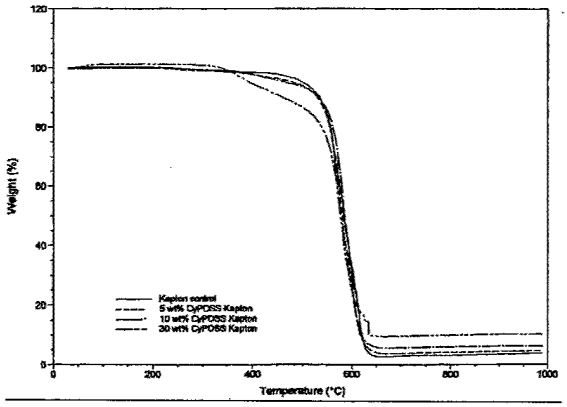


Fig. 5 . TGA for Kapton and POSS-Kapton polyimides under air, 10 °C/min heat ramp

Fig. 4 and Fig. 5 show thermal gravimetric analysis (TGA) charts of Kapton control and 5, 10 and 30 wt% POSS-polyimides under nitrogen and air purge respectively. As can be seen from Fig. 4, the onset of thermal degradation under a nitrogen atmosphere for the POSS containing polyimides begins at decreasing temperatures with increasing POSS content.

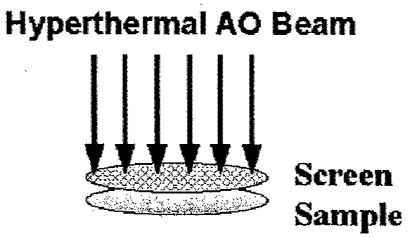


Fig. 6. AO etching experiment using a protective screen to shield selective areas of the sample for profilometry measurements

### 2.3 Profilometry and Atomic Oxygen Etching Experiments

Samples of POSS-Polyimide films underwent a series of AO etching experiments where they were exposed to an hyperthermal O-atom beam produced by a 7 Joule-pulsed $CO_2$ laser source. This AO source has been well characterized and described previously [12]. The resultant beam consists predominantly of fast neutrals, with a very small ionic fraction ($<10^4$). Average kinetic energies of the fast species in the beam can range from 2 to 15 eV.

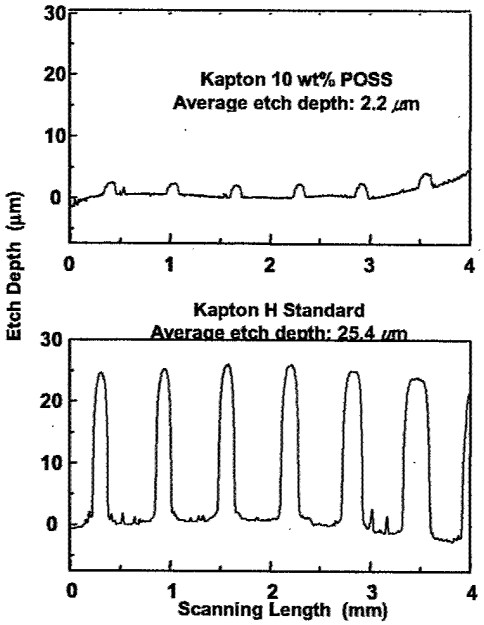


Fig. 7. Profilometry measurements obtained after a total AO fluence of $8.47 \times 10^{20}$ atoms/cm$^2$, equivalent to an approximate 10 day simulated LEO dosage

As depicted in Fig. 6, a protective screen was placed in-between the sample and beam path in order to

selectively erode only certain portions of the samples. The difference in etch depth between the eroded and protected part of the samples was then measured using stylus surface profilometry. Surface profilometry is a technique in which a diamond stylus, in contact with a sample, can measure minute physical surface variations as a function of position. It is commonly used to measure film thickness in thin film deposition and processing. By measuring the difference in height between the etched and unetched portions of the polymer sample, it is possible to calculate an AO reaction efficiency ($R_e$) or erosion rate for the material for a given flux. Profilometry measurements for the Kapton H standard and a 10 wt% POSS-Kapton polyimide sample are shown in Fig. 7 after a total fluence of $8.47 \times 10^{20}$ atoms/cm$^2$. This corresponds to 100,000 pulses of the laser atom source and correlates to an approximate 10 day simulated LEO dosage.

These measurements reveal that the average etch depth for the Kapton HN standard was 24.5 microns which corresponds to a calculated $R_e$ of $3.00 \times 10^{-24}$ cm$^3$/atom. This value agrees with previously reported erosion rates based on space flown and ground tested Kapton samples [13]. However, under the same conditions, the 10 wt% POSS-Kapton polyimide etched on average only 2.2 microns corresponding to an $R_e$ of $2.56 \times 10^{-25}$ cm$^3$/atom. It is interesting to note that this full order of magnitude improvement in atomic oxygen reaction efficiency is brought about by only a 10 wt % (approximately 1 mole%) addition of POSS copolymerized in the polymer matrix.

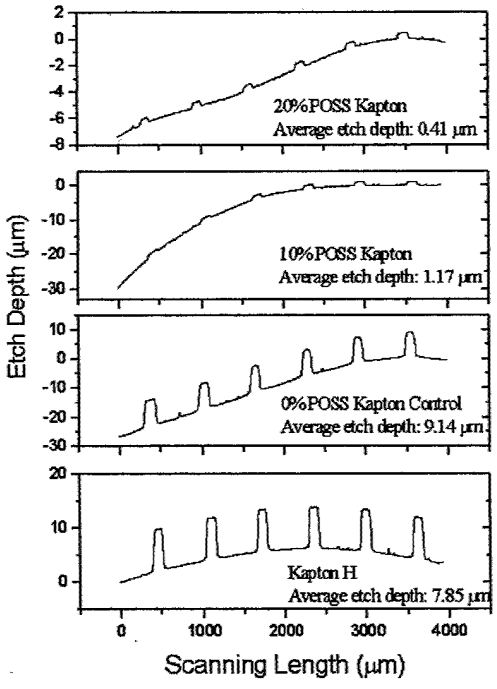


Fig. 8. Profilometry measurements obtained after a total AO fluence of $2.62 \times 10^{20}$ atoms/cm$^2$, equivalent to an approximate simulated 3 day LEO dosage

The experiment was repeated for a smaller AO fluence of $2.62 \times 10^{20}$ atoms/cm$^2$ exposing a commercially available Kapton H standard, a Kapton control sample with no POSS and a 10 and 20 wt% POSS-Kapton sample. Fig. 8 shows a multiplot of the profilometry measurements of these samples. The data for these plots reveal a decreasing average etch depth and corresponding atomic oxygen reaction efficiency as the POSS content in the polymer increases. Again, a full order magnitude improvement in the atomic oxygen reaction efficiency is obtained from addition of 10 wt% POSS, while addition of 20 wt% POSS improves the reaction efficiency by 22.5 times.

The superior performance of polyimides containing POSS is further highlighted by atomic force microscopy images before and after exposure to AO as shown in Fig. 10 and Fig. 11. These images reveal that the surface roughness increases dramatically for the Kapton control sample after AO exposure from 1.09 to 102 nm. In contrast, the surface roughness of the Kapton polyimides with POSS only slightly increases from 1.03 to 17.7 nm and from 1.55 to 6.75 nm for the 10 wt% and 20 wt% POSS respectively.

The protection provided to polyimides that contain POSS is actually much greater when looking at much longer exposure times. As can be seen in Fig. 9, erosion of the 10 and 20wt % POSS Kaptons to 400,000 AO beam pulses is drastically less than that of the Kapton control sample. This suggests that there is a equilibrium point where the surface is nearly completely protected from further AO attack resulting in negligible erosion. This is a result of the passivating and self-healing silica layer that is formed as a result of the nanodisperesed POSS moieties reacting with AO. This surface layer was characterized using X-ray photoelectron spectroscopy (XPS) as described below prevents further degradation of the underlying polymer.

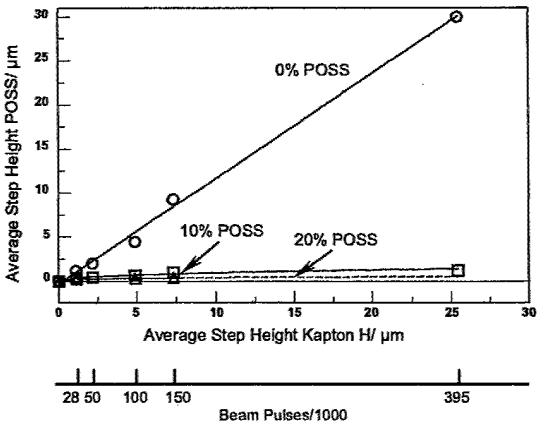


Figure 10. Erosion of Kapton and POSS Kapton versus AO beam pulses

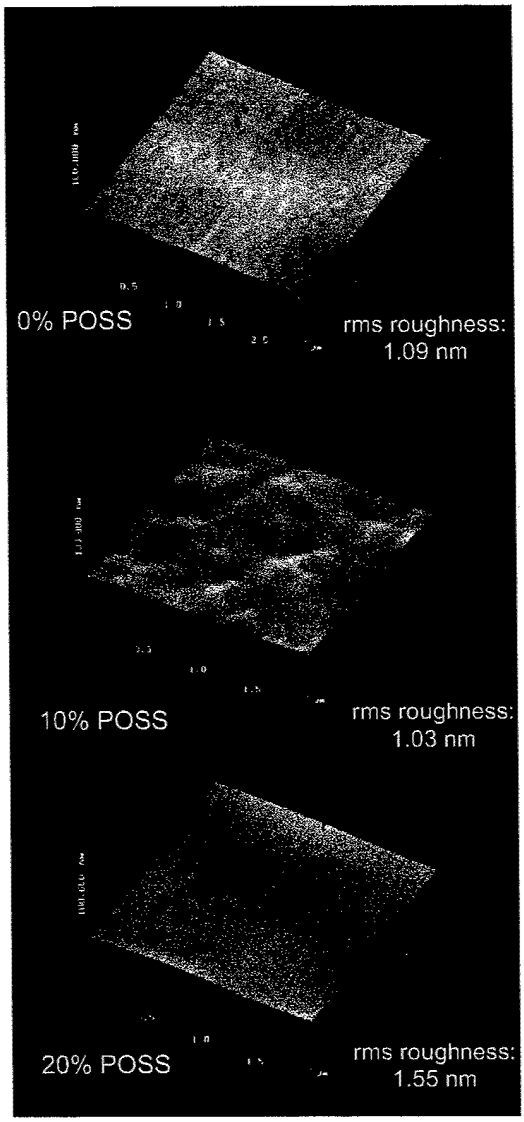


Fig. 10. Atomic Force Microscopy images of Kapton control and 10 and 20 wt% before exposure to AO

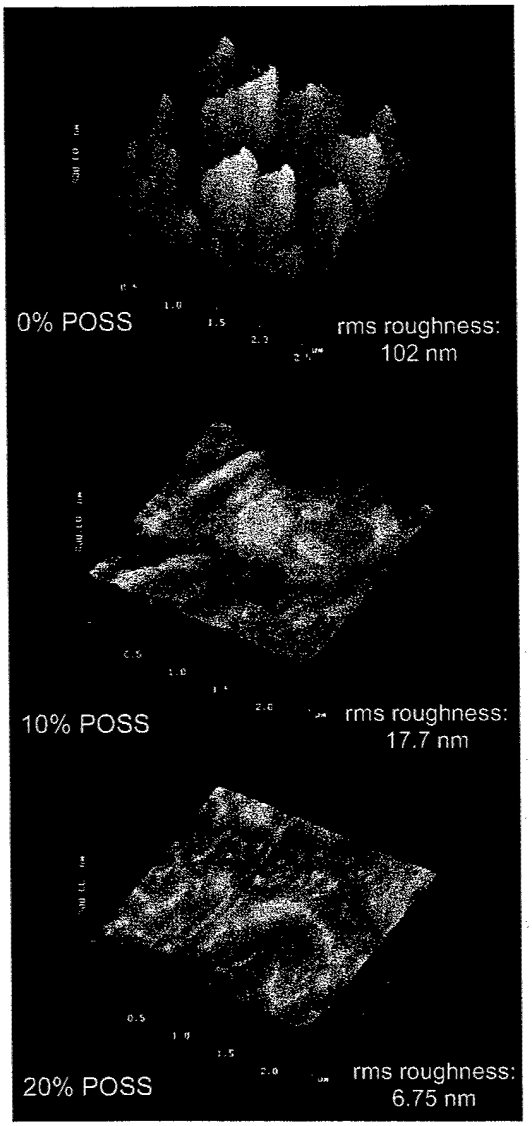


Fig. 11. Atomic Force Microscopy images of Kapton control and 10 and 20 wt% after a total AO fluence of $8.47 \times 10^{20}$ atoms/cm$^2$, equivalent to an approximate 10 day simulated LEO dosage

**2.4 In-situ XPS Analysis After Exposure to an ESD Atomic Oxygen Source**

A 10 wt% POSS-Polyimide film has been characterized in situ by using XPS before and after incremental exposures to the flux produced by an electron stimulated desorption (ESD) atomic oxygen source. This source, developed by Hoflund and Weaver [14], is ultrahigh vacuum (UHV) compatible, operates with the sample at room temperature and produces a high purity, hyperthermal AO flux with an O atom: $O^+$ ratio of ~$10^8$.

XPS spectra were first obtained from the as-entered, solvent-cleaned sample. The sample was then transferred into an adjoining UHV chamber that houses the atomic oxygen source via a magnetically coupled rotary/linear manipulator. There the surface was exposed to a hyperthermal AO flux and re-examined without air exposure after total exposure times of 2, 24, and 40 h. The approximate normal distance between the sample faces and source in this study was 15 cm, at which distance the flux was about $2.0 \times 10^{15}$ atoms/cm$^2$-s for the instrument settings used. The sample was maintained at room temperature during the AO exposures with a slight temperature increase to 50°C due to exposure to the X-ray source during XPS data collection. The substrate temperature was determined using a chromel-alumel thermocouple. After the 40 h AO exposure, the sample was exposed

to air (room temperature, ~22°C, relative humidity ~60%) and again examined using XPS.

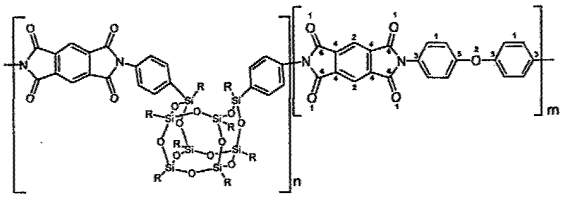

Fig. 12 Molecular structure of POSS-Kapton with numerically labeled atomic sites

The POSS-Kapton molecular structure with labeled atomic sites is shown in Fig. 12. XPS survey spectra obtained from a solvent-wiped 10 wt% POSS-polyimide surface before and after the 2, 24 and 40 h AO exposures and final air exposure are shown in Fig. 13. The peak assignments shown in Figure 12 pertain to all five spectra. The predominant peaks apparent in these spectra include the C 1s, N 1s, O 1s, Si 2p, Si 2s, O 2s and O Auger peaks. Significant changes in relative peak heights are observed for the C, O, and Si features following the O-atom exposures. XPS is a surface sensitive technique ideally suited for studying AO erosion of spacecraft materials. The outermost surface region which is affected to the greatest extent due to reaction with AO also makes the largest contribution to the XPS signal. The weighted average compositional values of the near-surface region determined using the homogeneous assumption are shown in Table 1 as a function of AO fluence. They provide a trend which is indicative of the chemical alterations occurring during AO exposure. This trend is supported by the chemical state alterations determined by XPS, which are discussed below.

Table 1. Near-surface composition determined from XPS data obtained from the as-entered, AO and air-exposed 10 wt% POSS-Polyimide sample

| Surface sample treatment | AO fluence O/cm$^2$ | Composition, at.% O | Si | C | N | O:Si ratio |
|---|---|---|---|---|---|---|
| As entered | ——— | 15.9 | 4.6 | 74.5 | 4.9 | 3.4 |
| 2 h r AO | $1.44\times10^{17}$ | 14.3 | 4.9 | 72.6 | 8.2 | 2.9 |
| 24 h AO | $1.77\times10^{18}$ | 11.1 | 4.4 | 79.6 | 4.9 | 2.5 |
| 40 h AO | $4.53\times10^{18}$ | 9.1 | 3.7 | 81.5 | 5.6 | 2.4 |
| Air exposed | $4.53\times10^{18}$ | 13.9 | 3.5 | 76.8 | 5.8 | 3.9 |

As can be seen in Fig. 13, the O 1s peak decreases significantly upon exposure to the AO beam. As a result, the O/Si atomic ratio of 3.4 for the as-entered sample, decreases gradually to 2.4 after the 40 h AO exposure. This reduction of the O/Si ratio is due to AO induced surface compositional changes resulting in the removal of carbonyl groups from the polymer chain and formation of a surface silica layer as shall be explained in the high resolution spectra that follow. After exposure to air, the O/Si atomic ratio increases to 3.9 corresponding to adsorption of species present in air. An overall increase is observed in the C concentration on the surface during increased exposure. Since the surface compositions presented in Table 1 are relative, it is expected that as the O concentration decreases the C and Si would increase.

High-resolution XPS C 1s, O 1s, N 1s and Si 2p spectra obtained from the as-received, solvent-wiped surface before and after the 2, 24 and 40 h O-atom exposures are shown in (a)-(d) of Fig. 14 through Fig. 17. Spectra (e) of these figures were obtained after the exposure to air following the 40 h AO exposure. Variations in peak shapes and positions are observed between the nonexposed, AO-exposed, and air-exposed surfaces, indicating that the chemical species distribution is altered by exposure to the AO flux and then to air. In addition, no surface charging of the sample was evident during the experiment as this would have altered the spectra resulting in a significant binding energy (BE) shift. Differential charging would have resulted in peak broadening or peak multiplicity, however, this was not observed in this study.

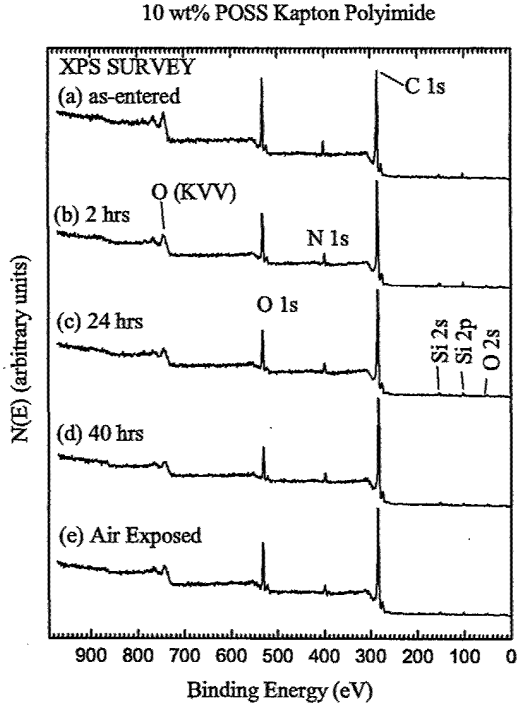


Fig. 13. XPS survey spectra obtained from a 10 wt% POSS-polyimide film as entered (a), after 2 h (b), 24 h (c), and 40 h exposure to the hyperthermal AO flux (d), and air exposure after the 40 h exposure (e)

The C 1s peak for the as entered sample in Fig. 14 is broad and centered at 284.7 eV indicating the predominant form of carbon present is aromatic. A high binding energy shoulder is present at 288.6 eV corresponding to the carbonyl carbon (6) in Fig. 12. However, as is also observed Kapton, this shoulder

diminishes upon exposure to AO. This is due to erosion of the carbonyl groups from the polymer backbone. This also results in a chemical state change of nitrogen on the surface as observed in the N 1s spectra in Fig 16.

The N 1s spectrum for the as entered sample is centered at 400.6 eV, corresponding to nitrogen bound as an imide functional group. However, as with regular Kapton, as the N-C=O bonds are broken upon removal of the carbonyl groups to form CO and $CO_2$, a lower binding energy shoulder begins to emerge in the N 1s spectra.

The chemical state changes in carbon and nitrogen associated with erosion also coincide with chemical state changes in the O 1s and Si 2p spectra in Fig. 16 and Fig. 17, which as with other POSS-polymers, reveal the formation of a silica layer on the outer surface. Upon inspection, it is evident from these spectra that a transition occurs for oxygen and silicon from a lower binding energy corresponding to the silsesquioxane to a higher binding energy and oxidation state associated with the formation of $SiO_2$ on the surface. These surface changes are presumably responsible for the reduced erosion rates and improved AO reaction efficiencies discussed presented herein.

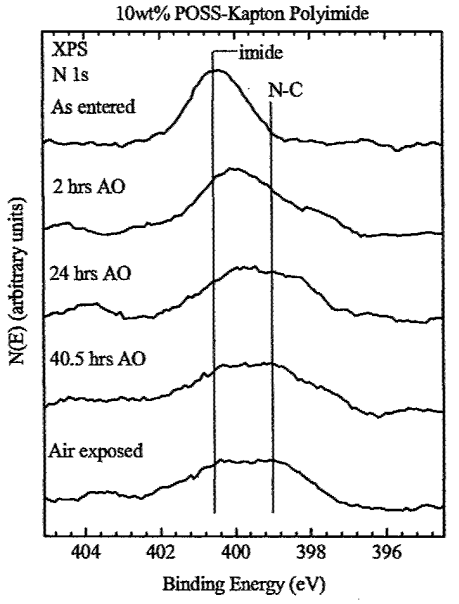


Fig. 15. XPS N 1s spectra obtained from a 10 wt% POSS-polyimide film as entered (a), after 2 h (b), 24 h (c), and 40 h exposure to the hyperthermal AO flux (d), and air exposure after the 40 h exposure (e)

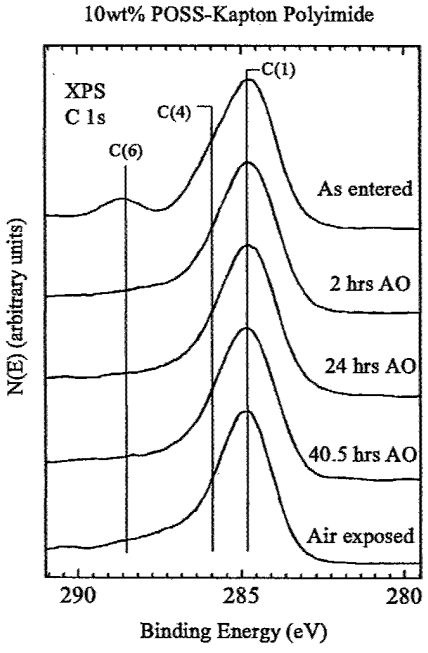


Fig. 14. XPS C 1s spectra obtained from a 10 wt% POSS-polyimide film as entered (a), after 2 h (b), 24 h (c), and 40 h exposure to the hyperthermal AO flux (d), and air exposure after the 40 h exposure (e)

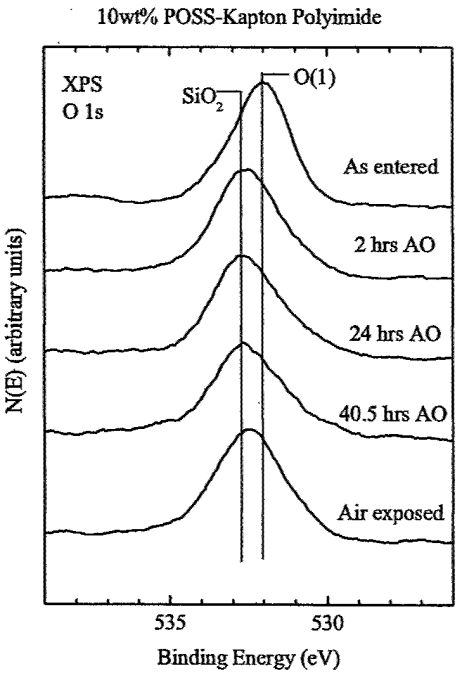


Fig 16. XPS O 1s spectra obtained from a 10 wt% POSS-polyimide as entered (a), after 2 h (b), 24 h (c), and 40 h exposure to the hyperthermal AO flux (d), and air exposure after the 40 h exposure (e)

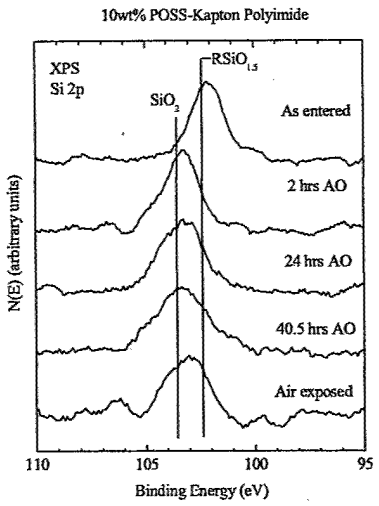


Fig. 17. XPS Si 2p spectra obtained from a 10 wt% POSS-polyimide film after insertion into the vacuum system (a), after 2 h (b), 24 h (c), and 40 h exposure to the hyperthermal AO flux (d), and air exposure after the 40 h exposure (e)

## 3. CONCLUDING REMARKS

The incorporation of POSS nanostructures into polyimides should significantly extend the usable lifetime of these materials in LEO applications. They exhibit a significantly improved oxidation resistance due to a rapidly formed ceramic-like, passivating and self-healing silica layer when exposed to high incident fluxes of atomic oxygen. The formed layer prevents further degradation of underlying virgin polymer. This technology could be easily adapted to other polymeric systems, such as structural polymers like polyethylene and polypropylene, revolutionizing the field of space-survivable materials

## 4. REFERENCES

1. Haddad, T.S. and Lichtenhan, J.D., "Hybrid Organic-Inorganic Thermoplastics: Styryl-Based Polyhedral Oligomeric Silsesquioxane Polymers," Macromolecules, 1996. 29(22): p. 7302-7304.

2. Lee, A. and Lichtenhan, J.D., "Viscoelastic Responses of POSS Reinforced Epoxy Systems," Macromolecules, 1998. 31(15): p. 4970-4974.

3. Mather, P.T., Jeon, H.G., Romo-Uribe, A., Haddad, T.S., and Lichtenhan, J.D., "Mechanical Relaxation and Microstructure of Poly(Norbornyl- POSS) Copolymers," Macromolecules, 1999. 32(4): p. 1194-1203.

4. Feher, F.J., Nguyen, F., Soulivong, D., and Ziller, J.W., "A New Route to Incompletely Condensed Silsesquioxanes: Acid- Mediated Cleavage and Rearrangement of (c-$C_6H_{11}$)(6)$Si_6O_9$ to C- 2-[(c-$C_6H_{11}$)(6)$Si_6O_8X_2$]," Chemical Communications, 1999(17): p. 1705-1706.

5. Feher, F.J., Terroba, R., and Ziller, J.W., "A New Route to Incompletely-Condensed Silsesquioxanes: Base- Mediated Cleavage of Polyhedral Oligosilsesquioxanes," Chemical Communications, 1999(22): p. 2309-2310.

6. Feher, F.J., Soulivong, D., and Eklund, A.G., "Controlled Cleavage of $R_8Si_8O_{12}$ Frameworks: A Revolutionary New Method for Manufacturing Precursors to Hybrid Inorganic-Organic Materials," Chemical Communications, 1998(3): p. 399-400.

7. Blanski, R.L., Phillips, S. H., Chaffee, K., Lichtenhan, J. D.,, Lee, A., and Geng, H.P., "The Preparation and Properties of Organic/Inorganic Hybrid Materials by Blending POSS into Organic Polymers," Polymer Preprints, 2000. 41(1): p. 585.

8. Gonzalez, R. I., "Synthesis and In-Situ Atomic Oxygen Erosion Studies of Space-Survivable Hybrid Organic/Inorganic POSS Polymers," Ph.D. Dissertation, Chem Eng Department, University of Florida, 2002. http://purl.fcla.edu/fcla/etd/UFE1000127

9. Gonzalez, R. I., Phillips, S. H., Hoflund, G. B., "In Situ Oxygen–Atom Erosion Study of polyhedral oligomeric silsesquioxane-Siloxane Copolymer," Journal of Spacecraft and Rockets, 2000, 37(4), p.463 - 467.

10. Hoflund, G. B., Gonzalez, R. I., Phillips, S. H., "In situ oxygen atom erosion study of a polyhedral oligomeric silsesquioxane– polyurethane copolymer," Journal of Adhesion Science Technology., 2001, 15(10), p. 1199 1211.

11. Wright, M. E., Schorzman, D. A., Feher, F.J., and Jin, R. Z., "Synthesis and Thermal Curing of Aryl-Ethynyl-Terminated *co*POSS Imide Oligomers: NewInorganic/Organic Hybrid Resins," Chemistry of Materials. 2003, *15*, 264-268

12. Minton, T. K., and Garton, D. J., "Dynamics of Atomic-Oxygen-Induced Polymer Degradation in Low-Earth Orbit," in *Advanced Series in Physical Chemistry: Chemical Dynamics in Extreme Environments*, edited by R. A. Dressler (World Scientific, Singapore, 2001), pp. 420-489.

13. Tennyson, R.C., "Atomic Oxygen Effects On Polymer-Based Materials," Canadian Journal of Physics, 1991. 69(8-9): p. 1190-1208.

14. Hoflund, G.B. and Weaver, J.F., "Performance-Characteristics of a Hyperthermal Oxygen-Atom Generator," Measurement Science & Technology, 1994. 5(3): p. 201-204.

# Synthesis and Atomic Oxygen Erosion Testing of Space-Survivable POSS (Polyhedral Oligomeric Silsesquioxane) Polyimides


9th International Conference on
Materials in a Space Environment
Noordwijk, The Netherlands, 16-20
June 2003

**Capt. Rene I. Gonzalez, Ph.D.**
**Project Leader**
**POSS-Polymer Working Group**
**Air Force Research Laboratory**
**(661)275-5252**
**rene.gonzalez@edwards.af.mil**



http://purl.fcla.edu/fcla/etd/UFE1000127

# Polymeric Materials

- Cost is the variable plaguing all space missions. ($5,000 to $10,000/1b to put payload in orbit)
- Materials are one of the main drivers of cost for space missions.
- Polymers offer many advantages (lightweight, easy to process, versatility)
- However, polymers are subject to severe degradation in Low Earth Orbit space environment

# LEO Environment (Altitudes of 200 to 1500 km)

- Atomic Oxygen
  - ~$10^8$ atoms/$cm^3$
  - Formed from photo-dissociation of $O_2$ in atmosphere.
  - Actual flux on spacecraft traveling at 8 to 12 km/s ~$10^{15}$ atoms/$cm^2$•s
  - collision energy ~ 5eV (C-C ~ 4 eV, C-N ~ 3 eV)
- Low-energy and high energy charged particles.
- Thermal cycling -50 to 150°C
- Solar UV and VUV radiation
  - VUV wavelengths in LEO extend below 290nm.
  - Bond scission and radical formation can lead to embrittlement.

# Goal: Develop Multi-Functional, Space-Survivable Materials

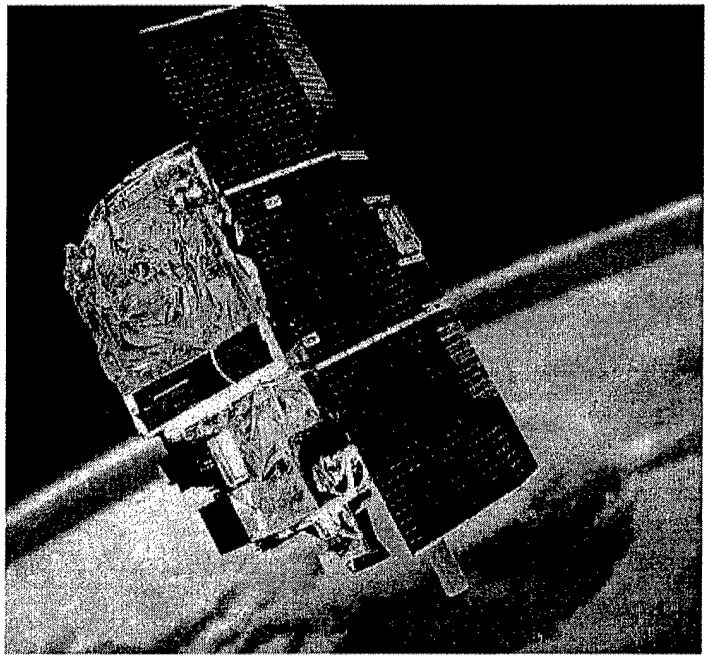

Satellites & Space Systems

| Atomic Oxygen Reaction Efficiency $cm^3$/atom | | |
|---|---|---|
| Material | Rel. Rates* | LEO |
| Kapton | 1 | $3.0 \times 10^{-24}$ |
| Polyethylene | 0.9 | $3.7 \times 10^{-24}$ |
| FEP Teflon | <0.03 | $<0.05 \times 10^{-24}$ |
| FEP Teflon (Solar Max) | 0.6 | $1.0 \times 10^{-24}$ |
| Siloxane-imide block copolymers(25% /75%) | 0.1 | $0.3 \times 10^{-24}$ |
| Epoxy | 0.6 | $1.7 \times 10^{-24}$ |

**Objectives**

- Increase Space Survivability (AO, particle & VUV radiation, thermal cycling) of Polymeric Materials

- Self-Passivating/Self-Rigidizing/Self-Healing based on Hybrid organic/ inorganic nanocomposite incorporation

# Goal: Develop Multi-Functional, Space-Survivable Materials

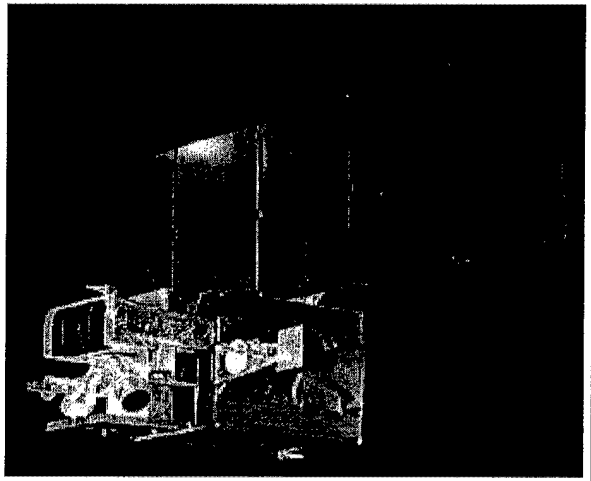

Satellites & Space Systems

| Bond | Dissociation Energy (EV) | λ (nm) | Material |
|---|---|---|---|
| $-C_6H_4-C(=O)-$ | 3.9 | 320 | Kapton® |
| C-N | 3.2 | 390 | Kapton® |
| $CF_3-CF_3$ | 4.3 | 290 | FEP Teflon® |
| $CF_2-F$ | 5.5 | 230 | FEP Teflon® |
| Si-O | 8.3 | 150 | Nanocomposite |
| Zr-O | 8.1 | 150 | Nanocomposite |
| Al-O | 5.3 | 230 | Nanocomposite |

## Objectives

- **Increase Space Resistance (AO, particle & VUV radiation, thermal cycling) of Polymeric Materials**
- **Self-Passivating/Self-Rigidizing/Self-Healing based on nanocomposite incorporation**

# Hybrid Inorganic/Organic Polymers

Goal: Develop High Performance Polymers that REDEFINE material properties

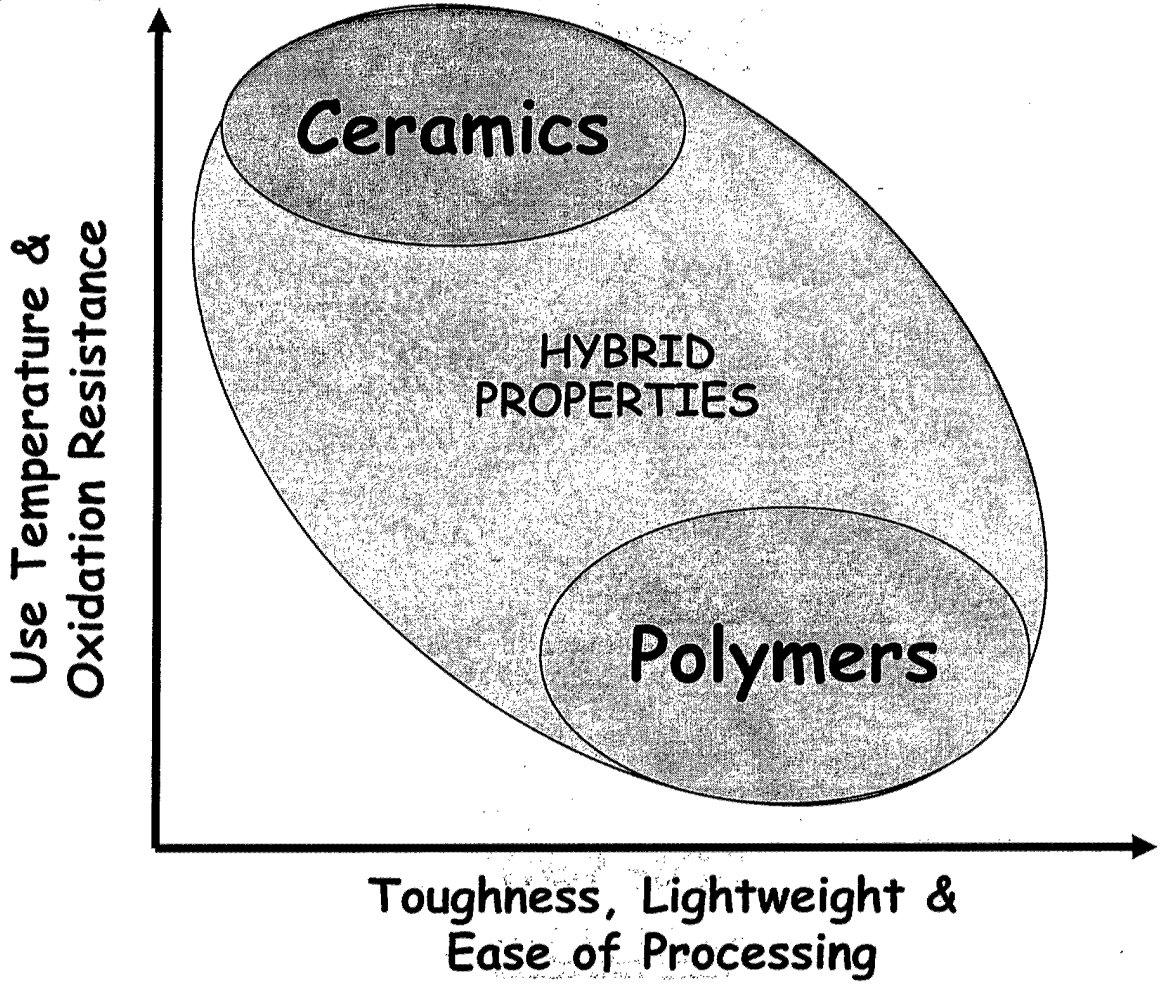


- Hybrid plastics bridge the differences between ceramics and polymers

# Polyhedral Oligomeric Silsesquioxanes (POSS) Synthesis

Hybrid Plastics™

$RSiX_3$ acid or base hydrolysis ⟶

**Blendables**

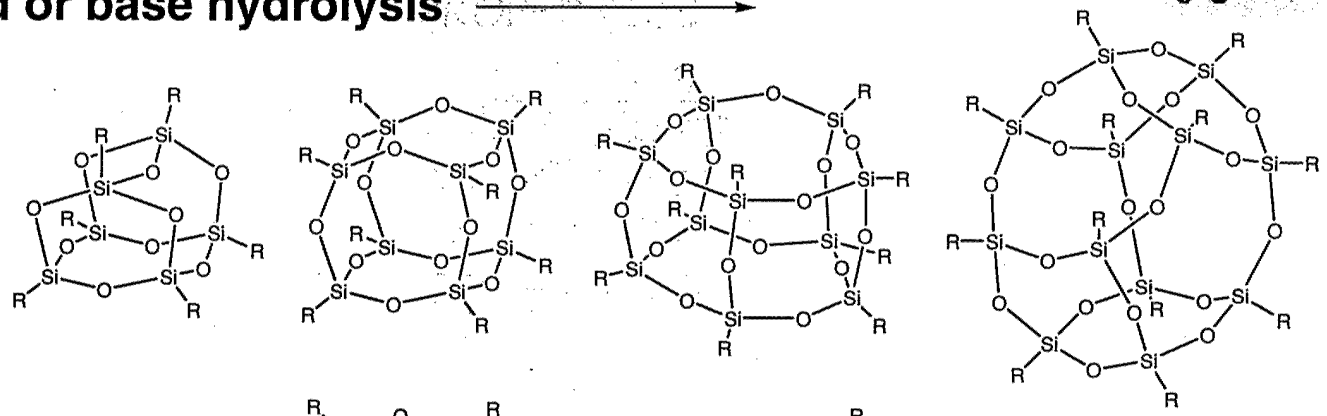

**Resin**

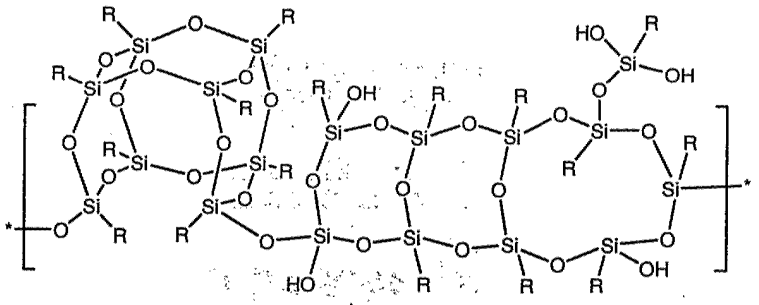

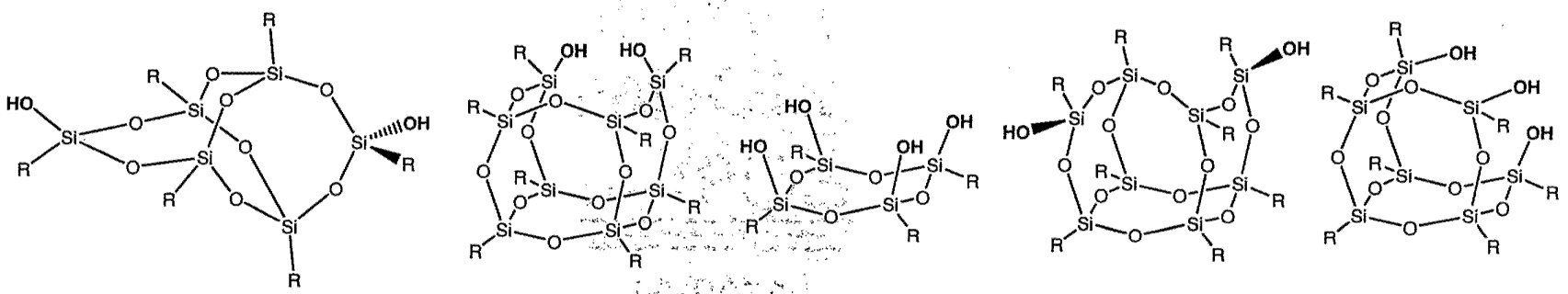

**Incompletely condensed cages**

Brown, Feher, AFRL, Hybrid Plastics

# Polymer Working Group - Research

**Basic R&D (6.1) PROGRAMS AFOSR**

**POSS Synthesis and Characterization**
**POSS Polymer Processing**
**POSS for Space-Survivable Materials**

**Applied R&D (6.2) PROGRAMS AFRL**

**Solid Rocket Motor Insulation/Casing**
**Liquid Rocket Engine Ducting**
**High Temp Lubes/Jet Canopies/Radomes**

**Technology Transfer**

# Anatomy of a POSS Nanostructure

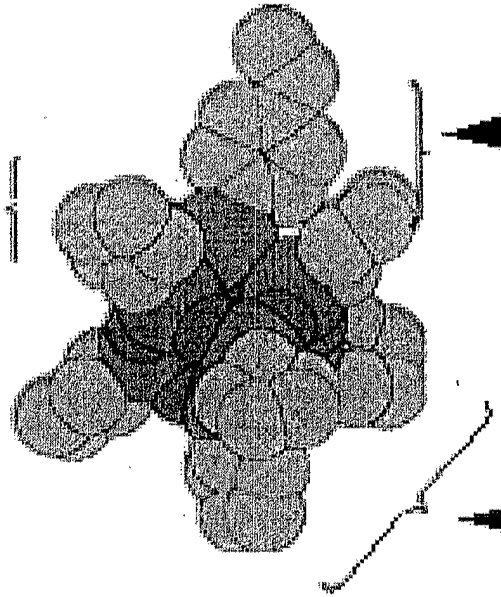

Nonreactive organic (R) groups for solubilization and compatibilization

Nanoscopic in size with an Si-Si distance of 0.5 nm and a R-R distance of 1.5 nm

May possess one or more functional groups suitable for polymerization or grafting.

Thermally and chemically robust hybrid (organic-inorganic) framework

Precise three-dimensional structure for molecular level reinforcement of polymer segments and coils.

# Why POSS and Why Nano?

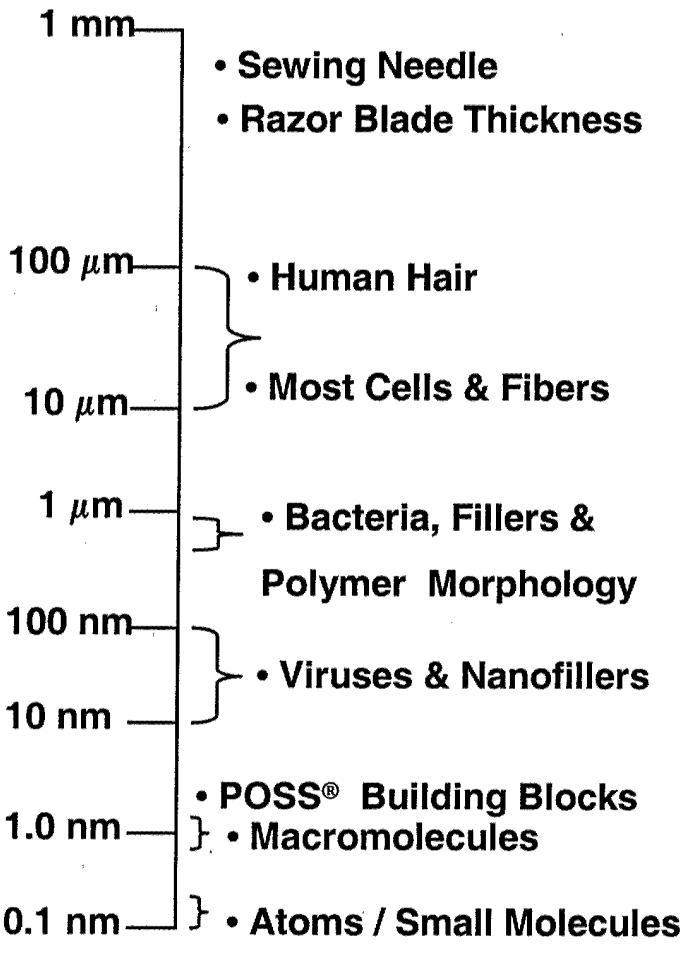


| Field | Property | Critical Length |
|---|---|---|
| **Electronics** | Tunneling | 1-100 nm |
| **Optical** | Quantum Well | 1-100 nm |
| | Wave Decay | 10-1000 nm |
| **Polymers** | Primary Structure | 0.1-10 nm |
| | Secondary Structure | 10-1000 nm |
| **Mechanics** | Dislocation Interaction | 1-1000 nm |
| | Crack Tip Radius | 1-100 nm |
| | Entanglement Rad. | 10-50 nm |
| **Therm-Mech.** | Chain Motion | 0.5-50 nm |
| **Nucleation** | Defect | 0.1-10 nm |
| | Critical Nucleus Size | 1-10 nm |
| | Surface Corrugation | 1-10 nm |
| **Catalysis** | Surface Topology | 1-10 nm |
| **Biology** | Cell Walls | 1-100 nm |
| **Membranes** | Porosity Control | 0.1-5 nm |

# POSS Polymer Incorporation

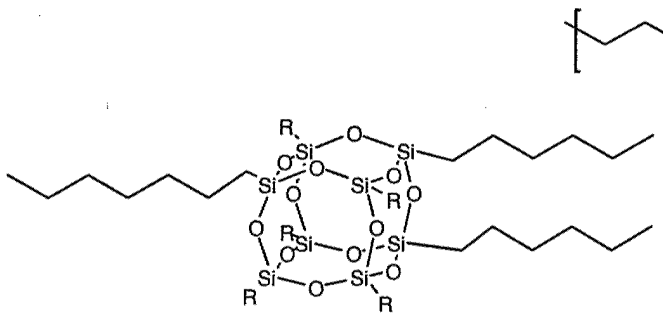

Cross-linker

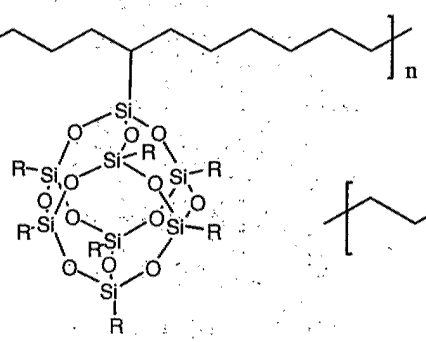

Pendant Polymer

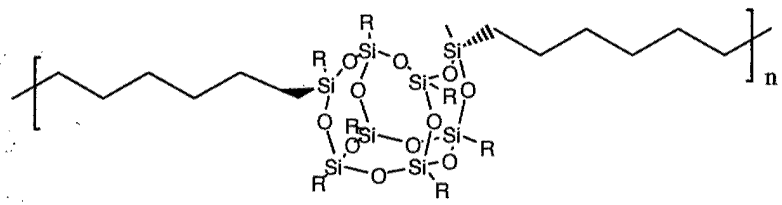

Bead Copolymer

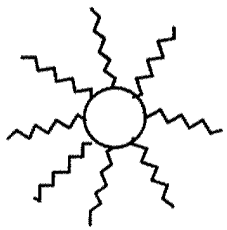

POSS Blending

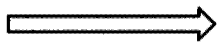

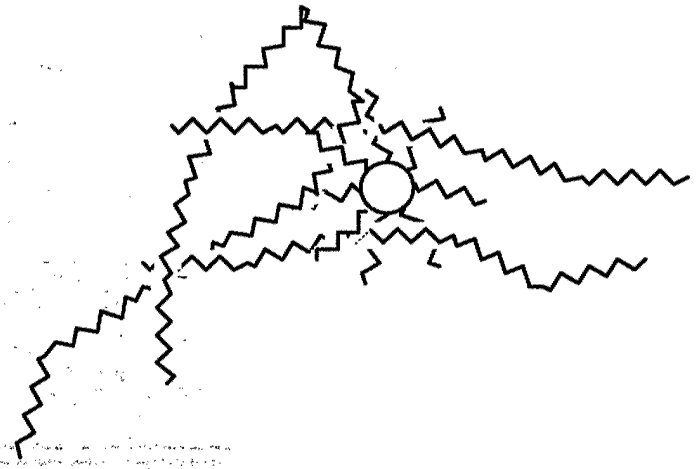

# POSS Macromers For Nanocomposites

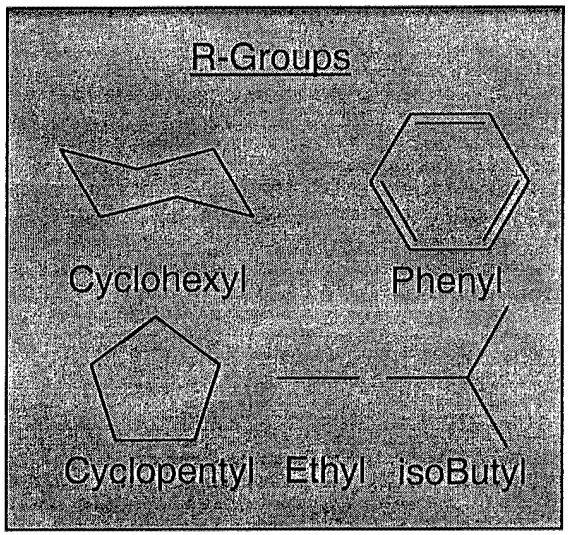


## Completely New Polymer Feedstock Technology

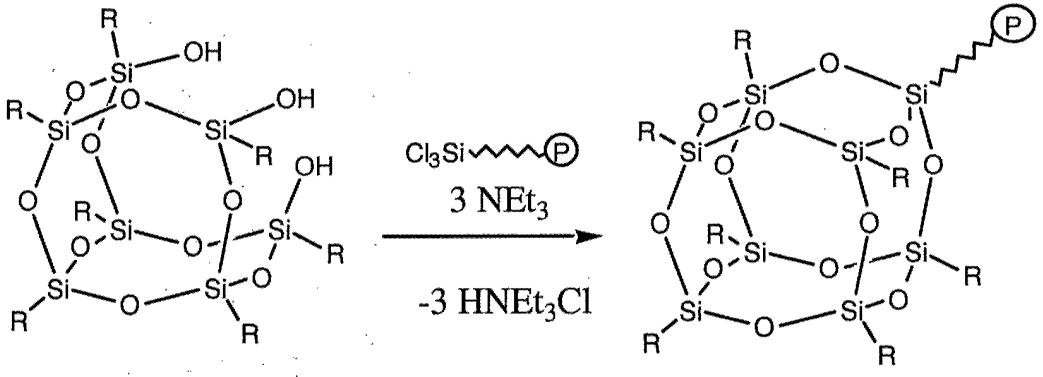


| | | | |
|---|---|---|---|
| Halides | Nitriles | Silanes | Styryls |
| Alcohols | Amines | Silanols | a-olefins |
| Esters | Isocyanates | Silylchlorides | Acrylics |
| Bisphenols | Epoxides | | Norbornenyls |

POSS-based macromers are available through either **Gelest** or **Aldrich**

POSS technology is commercialized by **Hybrid Plastics** in Fountain Valley CA

# Importance of R groups: Affect compatibility with polymer matrix

## 50 Wt % POSS Blends in 2 Million MW PS

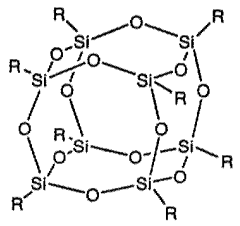

R = cyclopentyl

$Cp_8T_8$

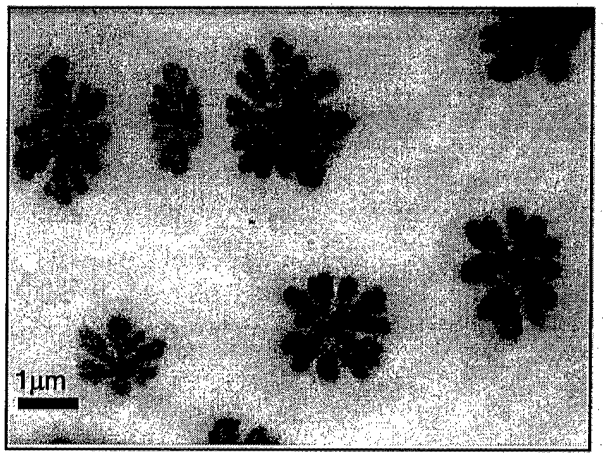


Domain Formation

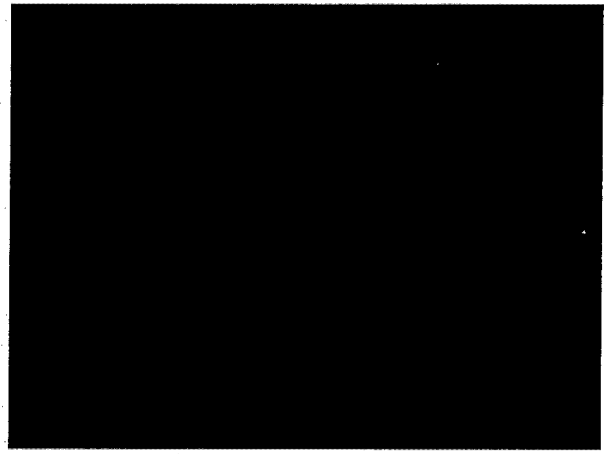

Partial Compatibility

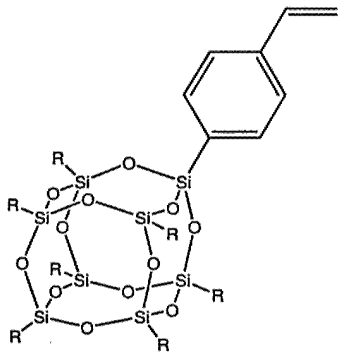

R = cyclopentyl

$Cp_7T_8Styryl$

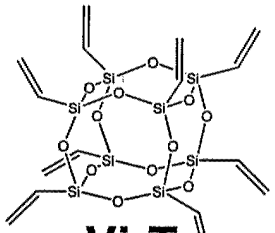

$Vi_8T_8$

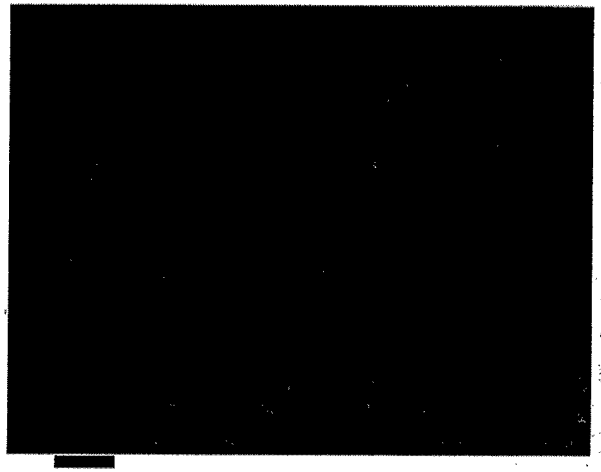

Immiscible POSS Crystallites

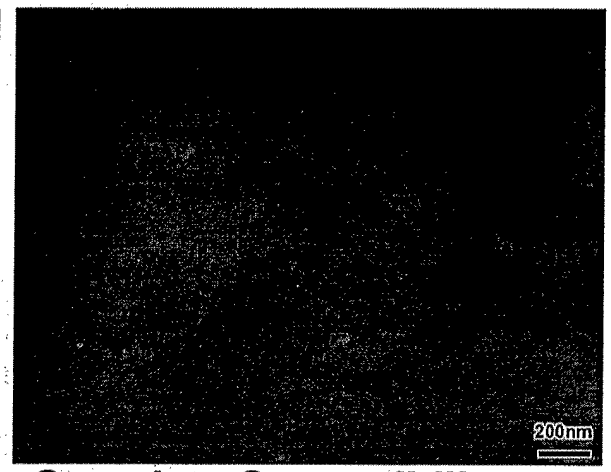


Complete Compatibility-
POSS Nanodispersion/Transparent

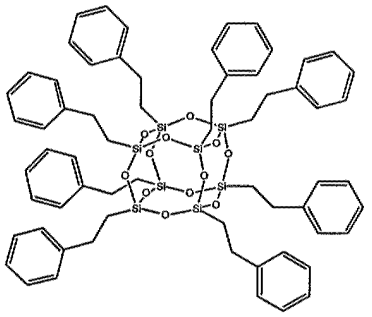

$Phenethyl_8T_8$

Blanski, et al., *Polymer Preprints*, **2000**. 41(1): p. 585.

# Polypropylene and $Methyl_8T_8$

**POSS Drop Test**
**Me8T8/i-PP**
**Dr. R. Blanski,**
**AFRL**
**Test Duration:**
**15:01**
**Time Lapse 20X**
**8 Feb 2001**

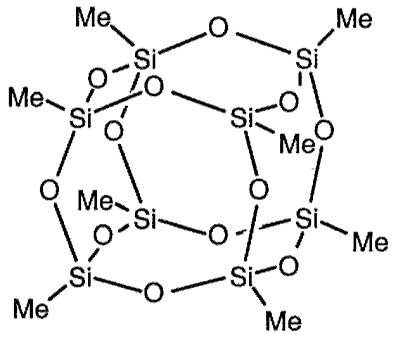


- Test run at 190 ˚C
- 1 Kg weight
- 10% POSS gave a 28 % improvement

# AO undercutting of LDEF Aluminized-Kapton Multilayer Insulation

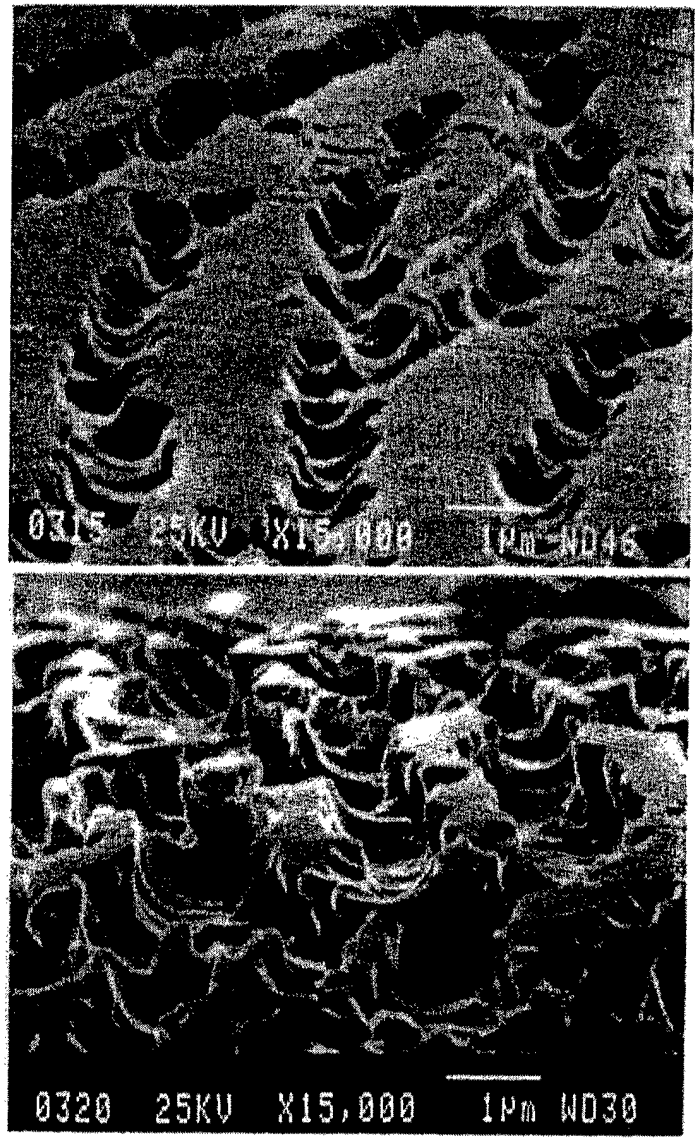


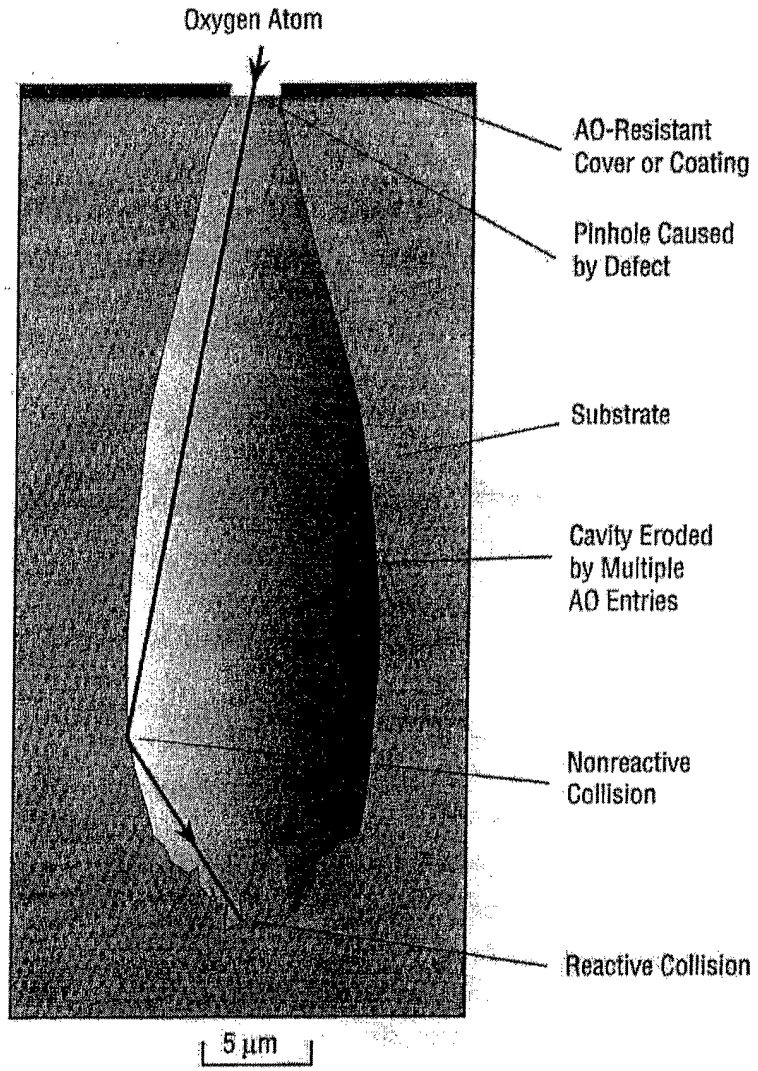


DeGroh, K.K., Banks, B.A., J. Spacecraft and Rockets, Vol. 31, No. 4, 656-664 (1994)

# Siloxanes

- **Siloxanes systems exhibit superior resistance to AO**
  - **High Si-O bond strength ~ 8 eV (C-C ~ 4 eV, C-N ~ 3 eV)**
  - **Oxyphilicity**

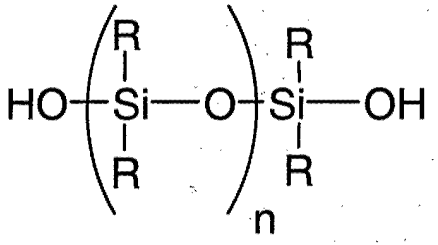


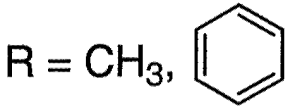


- **However, pure siloxane systems have disadvantages**
  - **Chain Scission**
  - **Volatile cyclic species which recondense on optical surfaces**

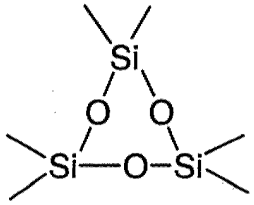


Cyclo($Me_2SiO)_3$

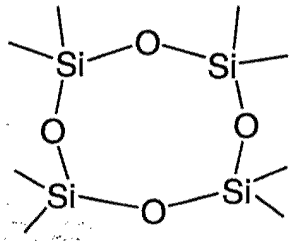


Cyclo($Me_2SiO)_4$

Cyclo($Me_2SiO)_5$

Cyclo($Me_2SiO)_6$

Cyclo($Me_2SiO)_7$

# LEO Simulation Facility

UNIVERSITY OF FLORIDA

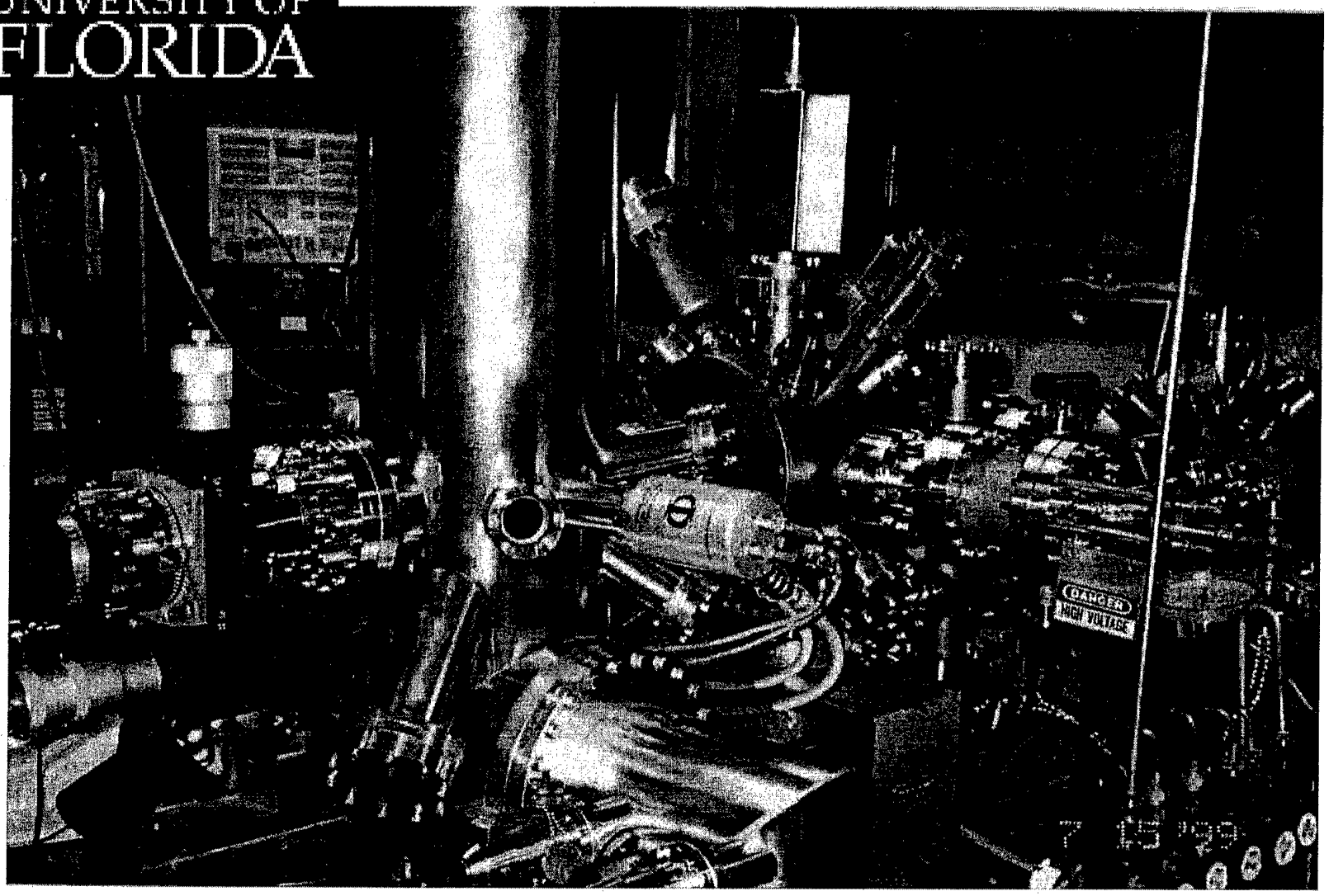

UNIVERSITY OF FLORIDA

# Oxygen Atom Source

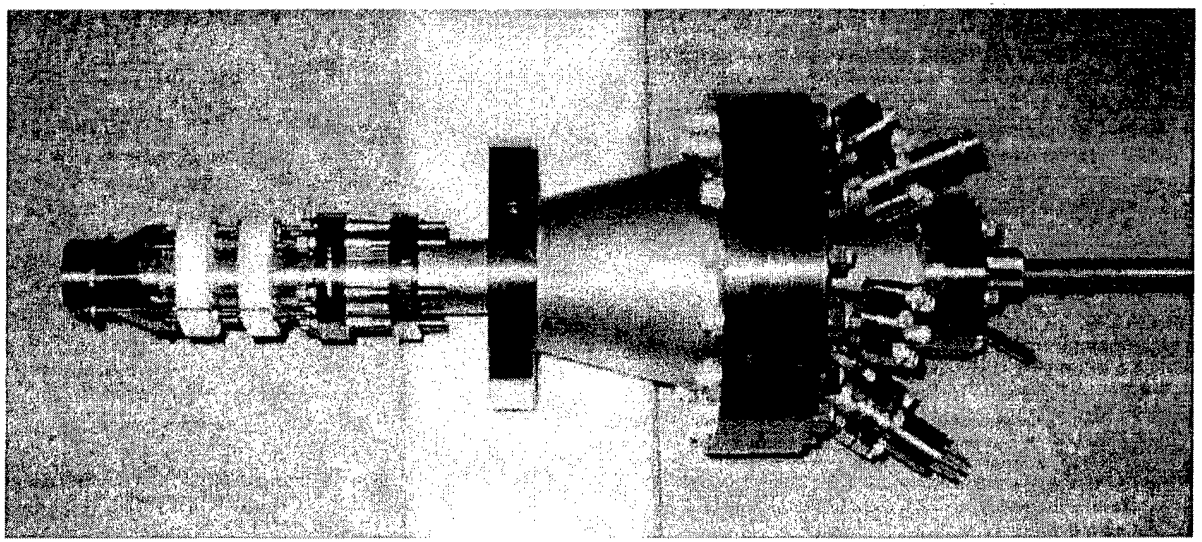

1. **Adsorption**
   **-maximize pressure**

2. **Permeation**
   **-membrane thickness**
   **-temperature**

3. **Desorption (ESD)**
   **-electron current**
   **-N adsorbed neutrals**

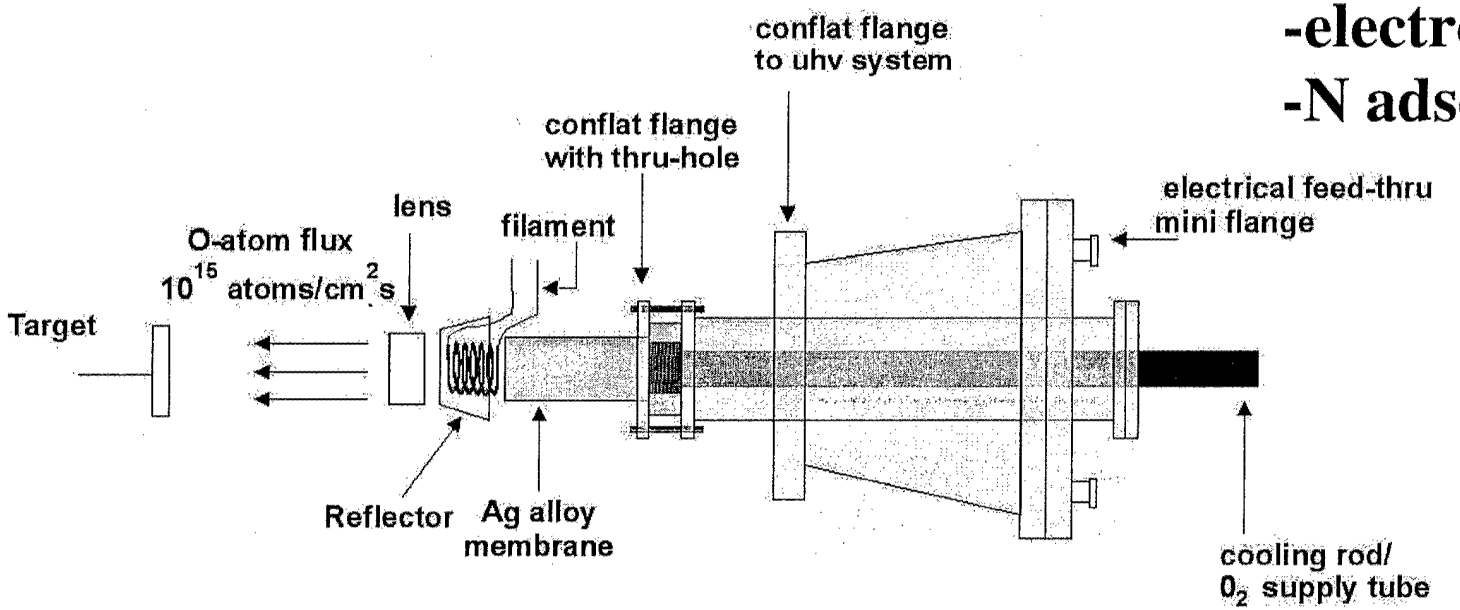

# POSS-Siloxane

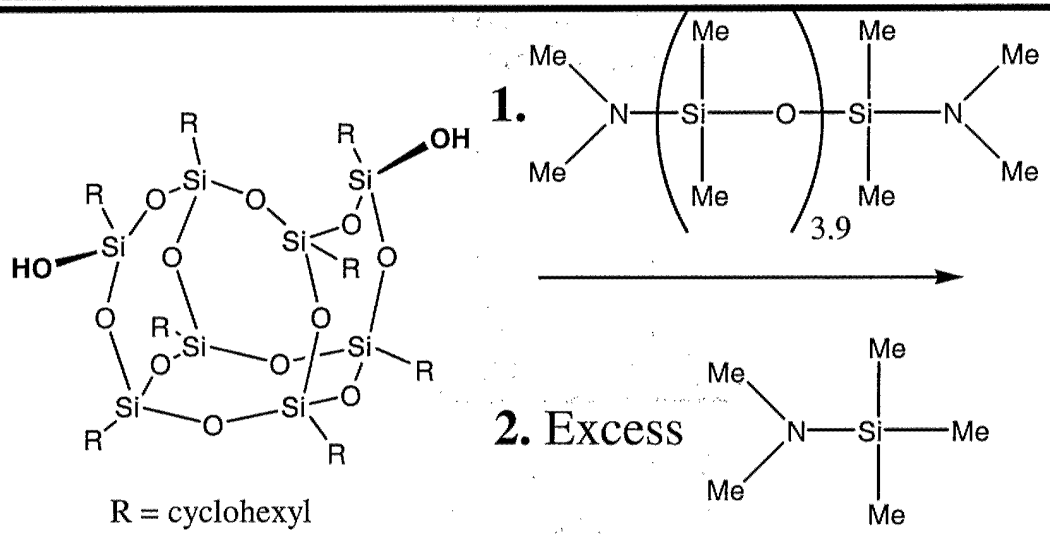


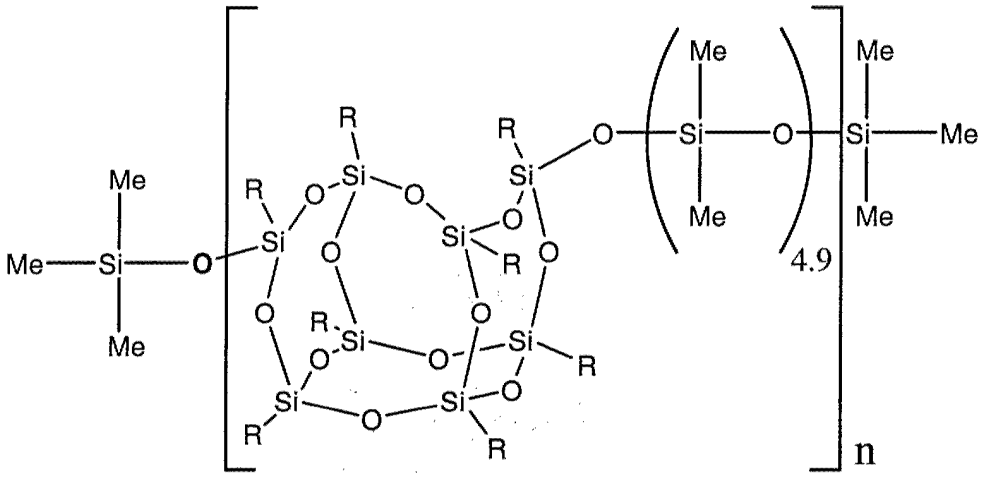


**POSS-PDMS Copolymer**

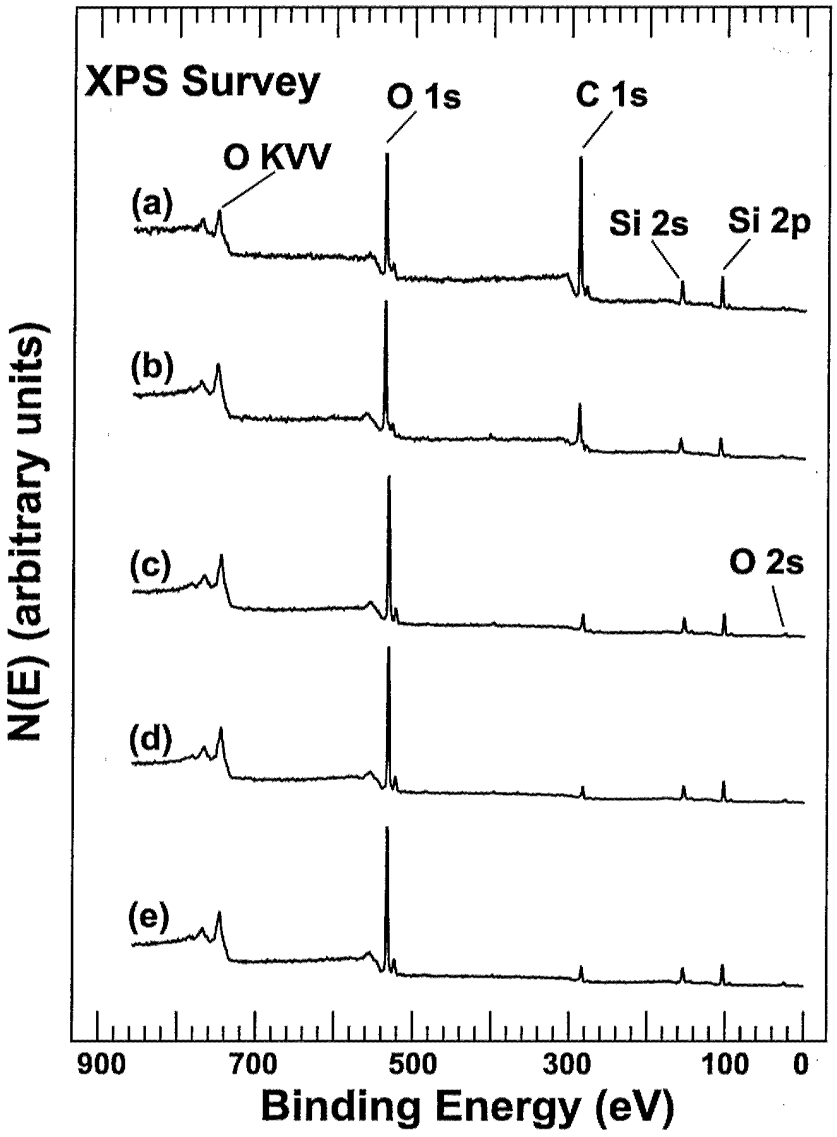


## POSS Siloxane

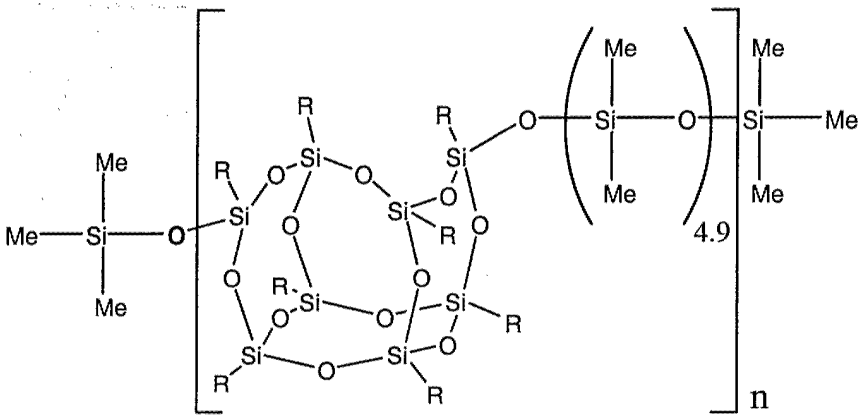


## Composition, at %

| Sample Treatment | O | C | Si |
|---|---|---|---|
| As entered | 18.5 | 65.0 | 16.6 |
| 2.0 hr | 33.8 | 48.4 | 17.8 |
| 24.6 hr | 49.1 | 22.1 | 28.8 |
| 63.0 hr | 55.7 | 16.3 | 28.0 |
| 4.8 hr air | 52.8 | 19.5 | 27.7 |

Gonzalez, R. I., Phillips, S. H., Hoflund, G. B., *J. of Spacecraft and Rockets*, Vol 37, No. 4, **2000**, pp. 463-467.

**XPS survey spectra obtained from a solvent-cleaned, POSS-PDMS film (a) after insertion into the vacuum system, (b), after a 2-hr (c) 24.6-hr and (d) 63-hr exposure to the hyperthermal AO flux, and (e) 4.75-hr air exposure following the 63-hr AO exposure.**

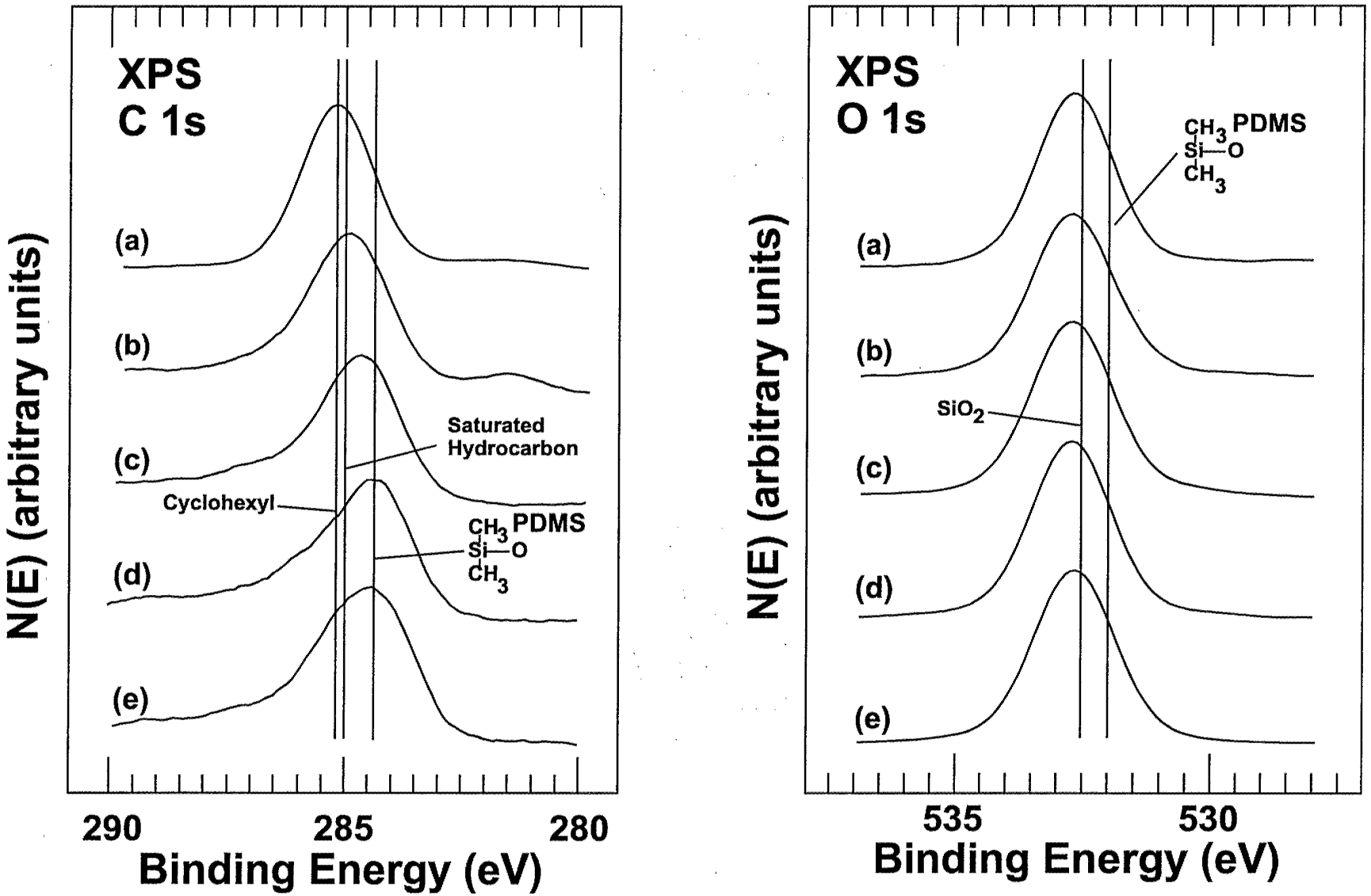


High Resolution C 1s and O 1s spectra obtained from a solvent-cleaned, POSS-PDMS film (a) after insertion into the vacuum system, (b), after a 2-hr (c) 24.6-hr and (d) 63-hr exposure to the hyperthermal AO flux, and (e) 4.75-hr air exposure following the 63-hr AO exposure.

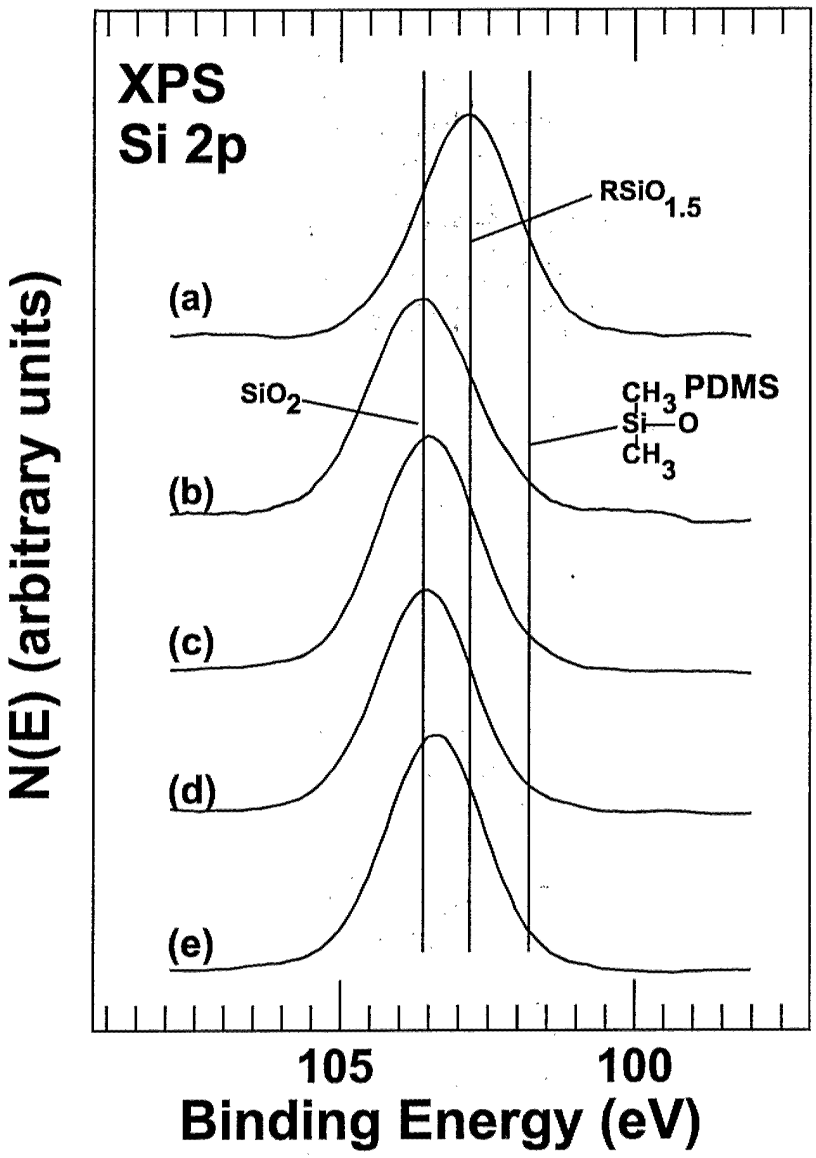


High Resolution Si 2p spectra obtained from a solvent-cleaned, POSS-PDMS film (a) after insertion into the vacuum system, (b), after a 2-hr (c) 24.6-hr and (d) 63-hr exposure to the hyperthermal AO flux, and (e) 4.75-hr air exposure following the 63-hr AO exposure.

# SEM of POSS-Siloxane Copolymer

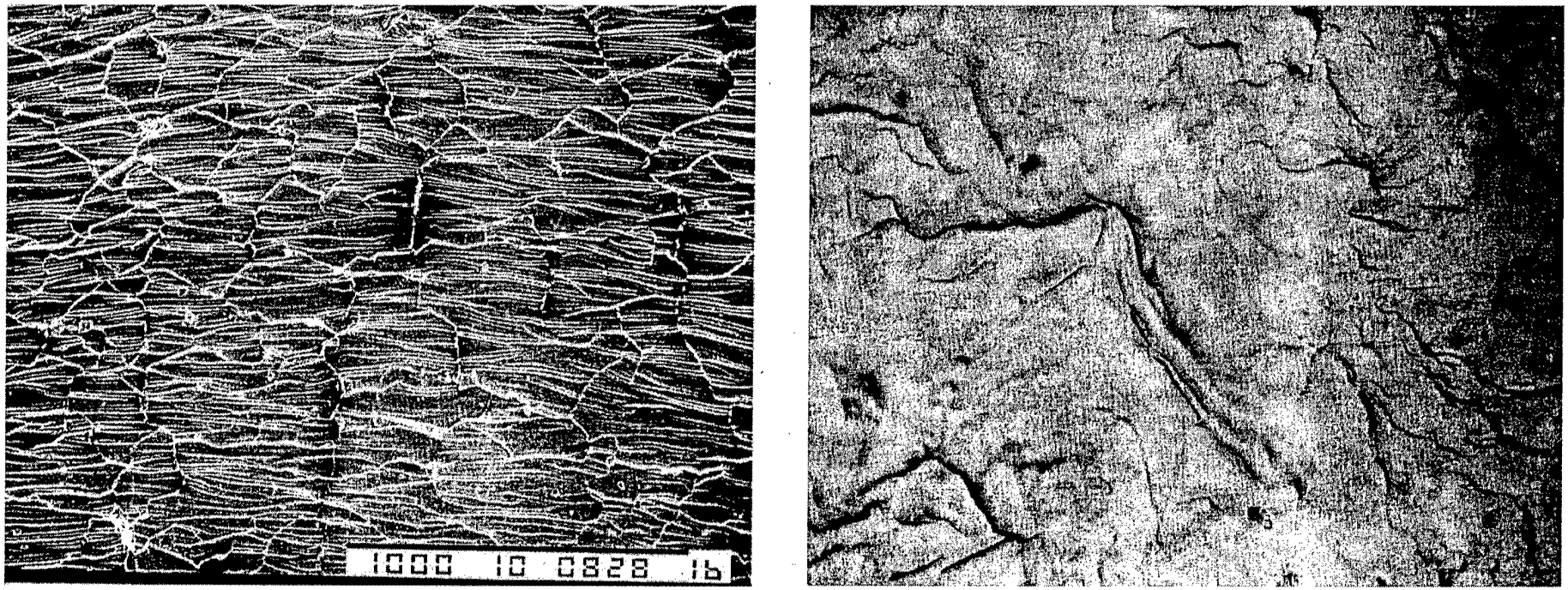


SEM of (a) unexposed and (b) exposed POSS-siloxane copolymer surfaces. The simulated LEO exposure "healed" the micro-cracks present initially in the POSS-siloxane sample.

Gilman, J.W., Shlitzer, D.S., Lichtenhan, J.D.; J. Appl. Polymer Sci., 60, 591-596 (199

# POSS-Polyurethane

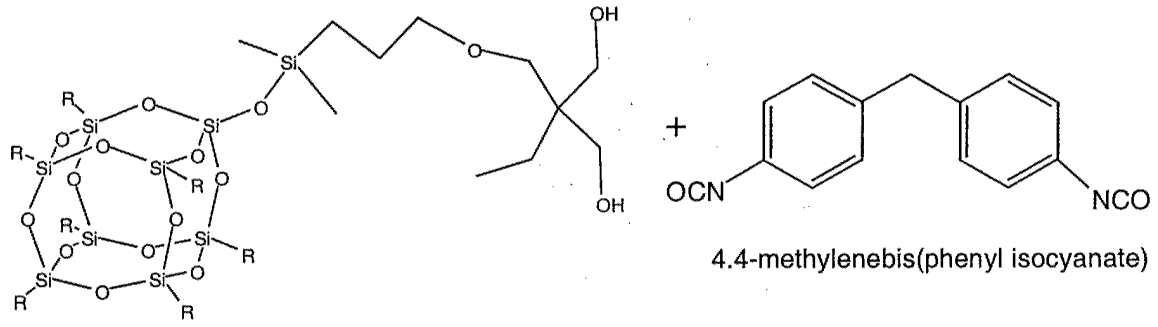


4.4-methylenebis(phenyl isocyanate)

R = cyclopentyl

POSS-TMP diol

$Et_3N$/DBTDL
PTMG ($M_n$=2000)
1,4-butanediol

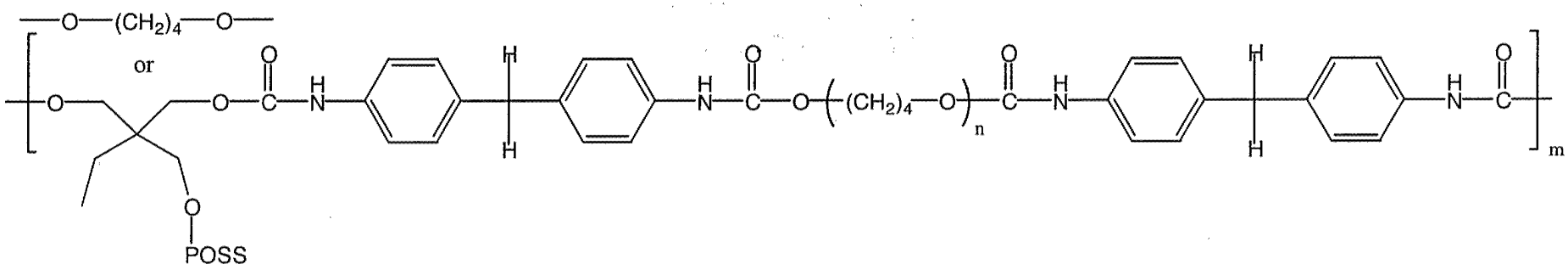



Fu, B.X., et al. *High Performance Polymers*, **2000**. 12(4): p. 565-571.

Fu, B.X., et al. *Polymer*, **2001**. 42(2): p. 599-611.

# 60 wt % POSS-Polyurethane

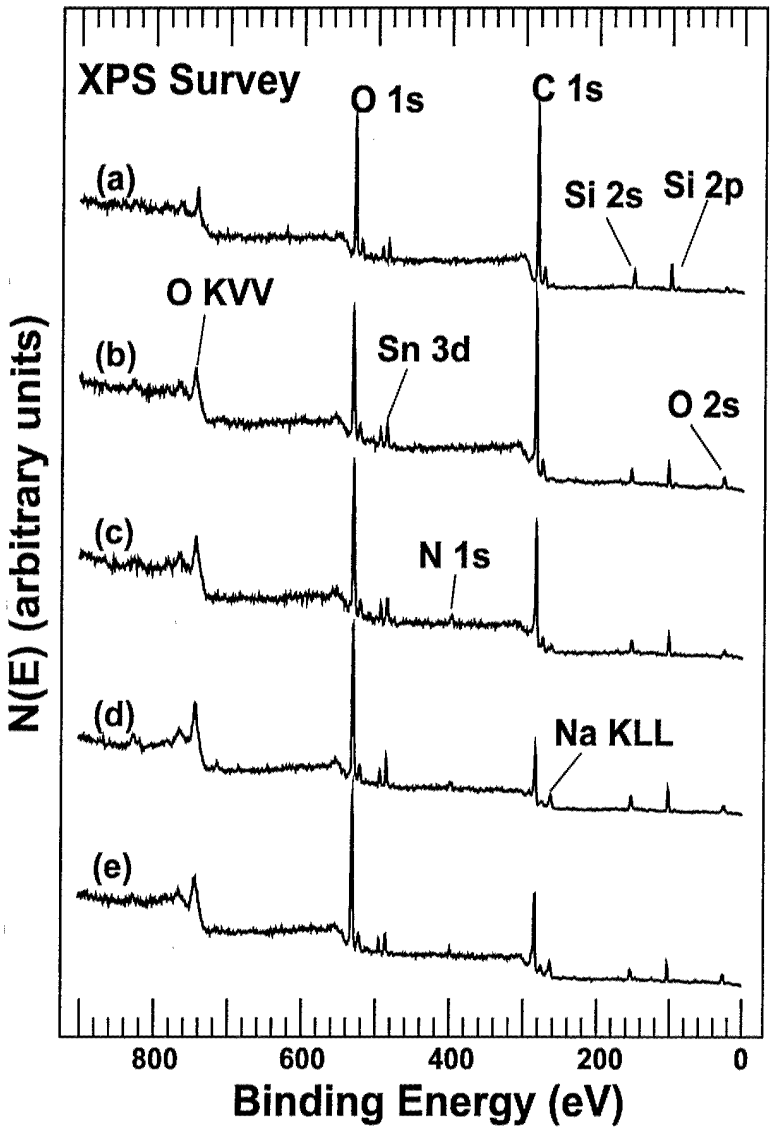


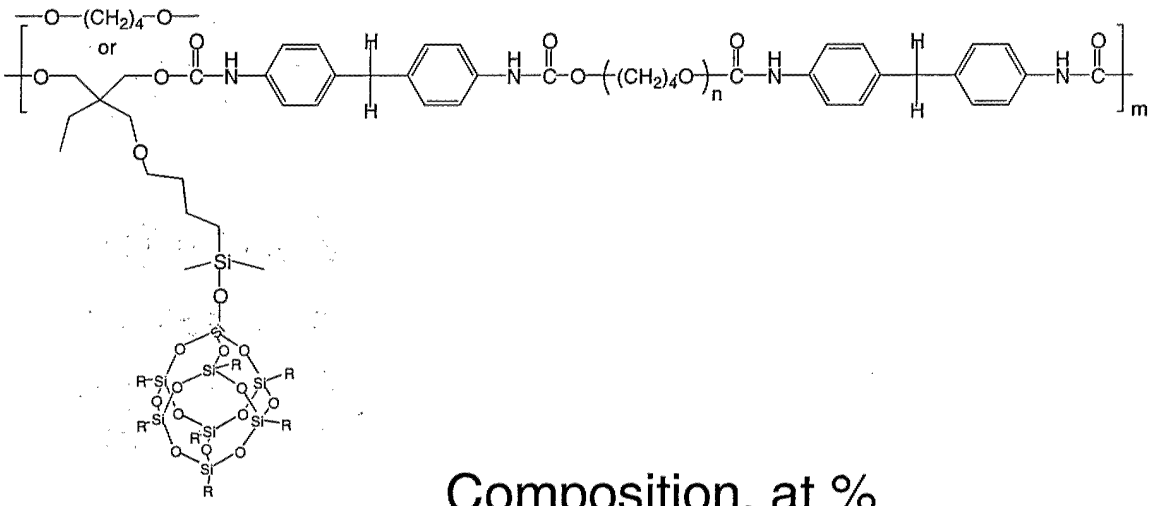


## Composition, at %

| Sample Treatment | O | C | Si | Sn | Na | N |
|---|---|---|---|---|---|---|
| As entered | 18.2 | 70.1 | 11.3 | 0.4 | - | - |
| 2.0-hr | 17.5 | 70.2 | 11.2 | 0.7 | 0.4 | - |
| 24.0-hr | 23.7 | 58.2 | 13.2 | 0.9 | 1.4 | 2.6 |
| 63.0-hr | 35.3 | 37.3 | 20.4 | 1.3 | 3.0 | 2.7 |
| 3.3-h air | 31.6 | 48.5 | 14.6 | 1.0 | 2.7 | 1.6 |

Phillips, S. H., Hoflund, G. B., Gonzalez, R. I., 45th International SAMPE Symposium, 2000, Vol. 45, No. 2, pp. 1921-1931.

**XPS Survey Spectra from a 60 wt% POSS-PU (a) after insertion into the vacuum system, (b) after a 2-hr (c) 24-hr and (d) 63-hr exposure to the hyperthermal AO flux, and (e) 3.3-hr air exposure following the 63-hr exposure.**

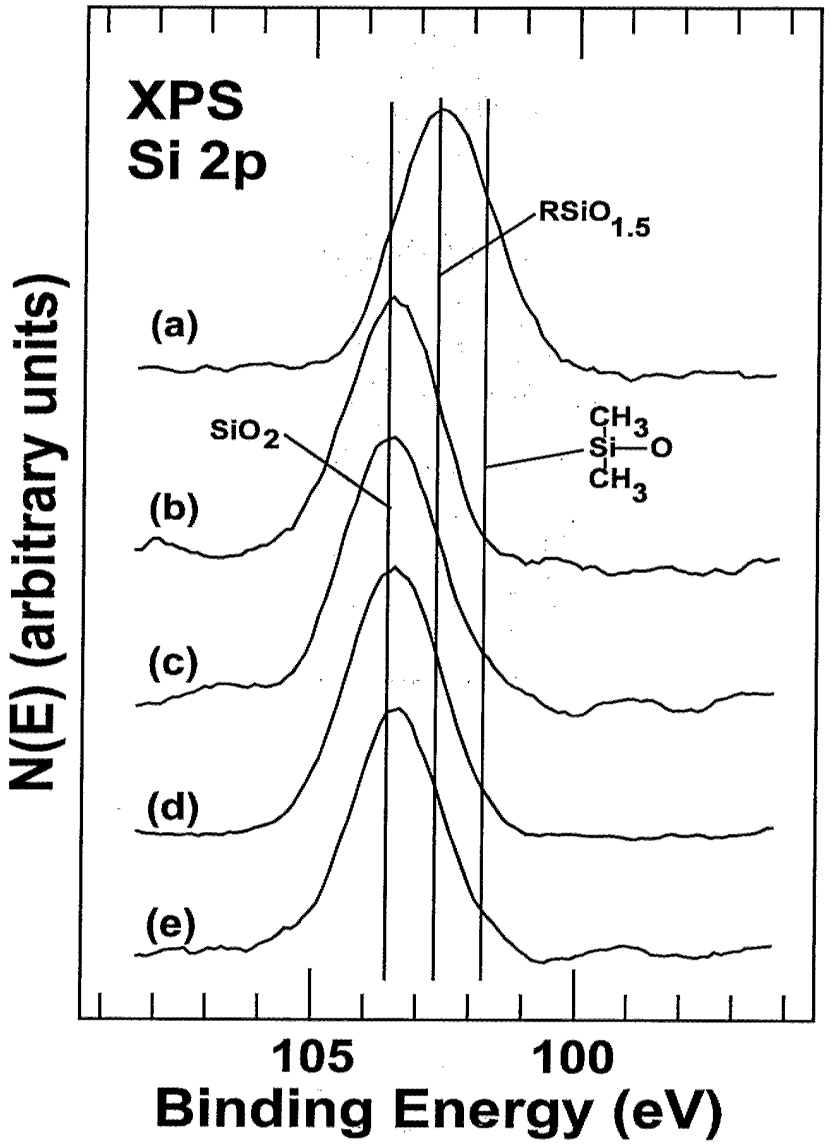


High Resolution Si 2p spectra from a 60 wt% POSS-PU (a) after insertion into the vacuum system, (b) after a 2-hr (c) 24-hr and (d) 63-hr exposure to the hyperthermal AO flux, and (e) 3.3-hr air exposure following the 63-hr exposure.

# Kapton

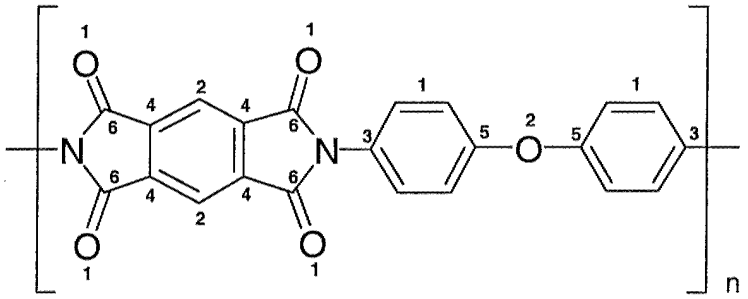

**3.0 x $10^{-24}$ $cm^3$/atom**

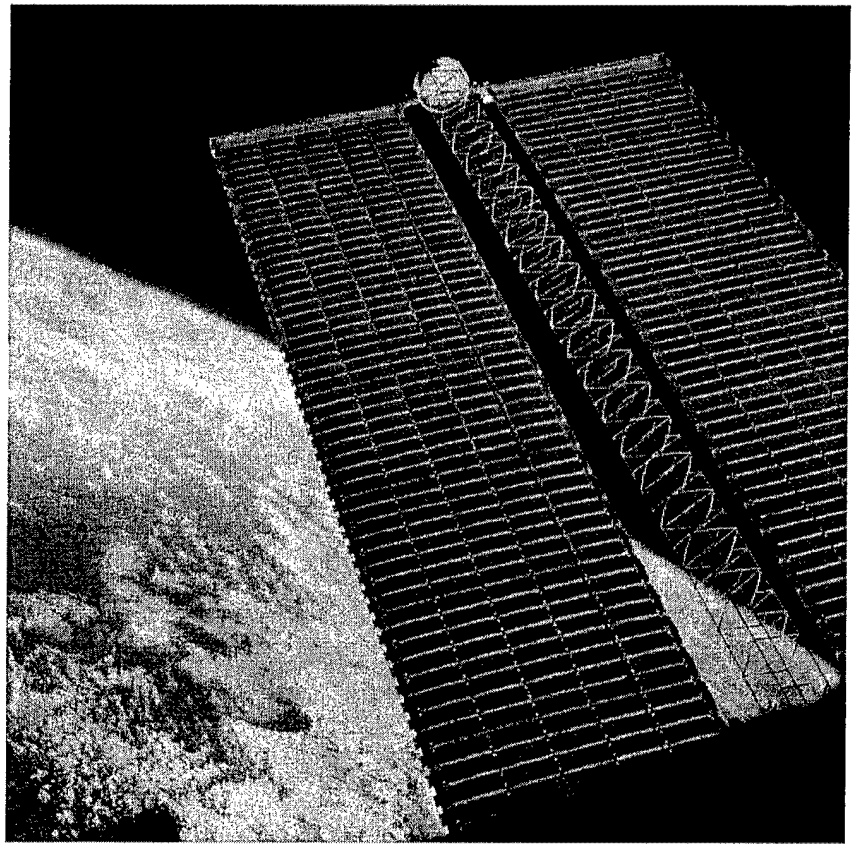

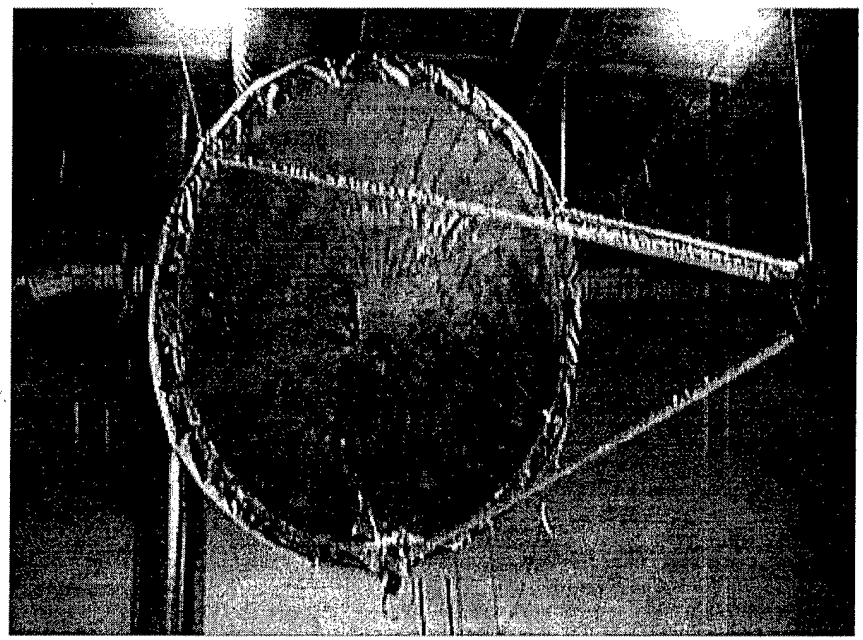

**Solar arrays**
**Space inflatable structures**

**Superior optical properties, low solar absorptance, high thermal reflectance**

**Excellent mechanical thermal properties**

# First POSS-Aniline Synthesis

**Multiple step synthesis**
**Moisture and air sensitive**
**Not amenable to scale up**

**Yet Critical for Development of POSS-polyimides!!!**

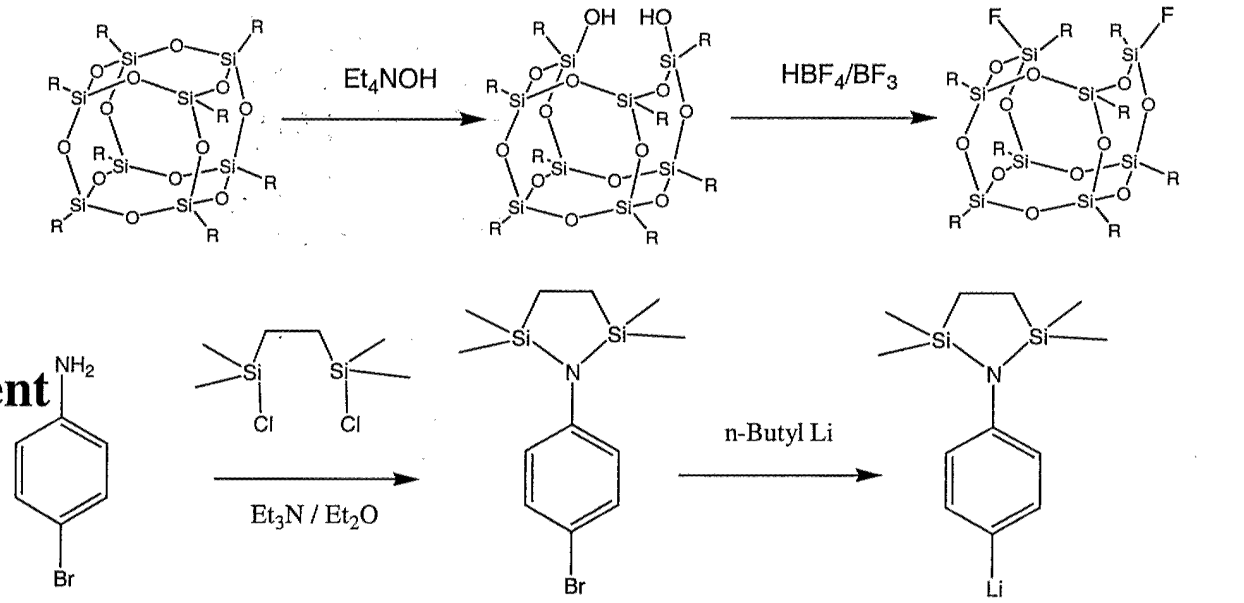

# POSS-Kapton Polyimides

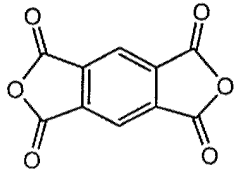

PMDA

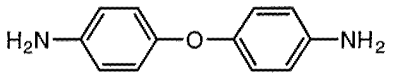

ODA

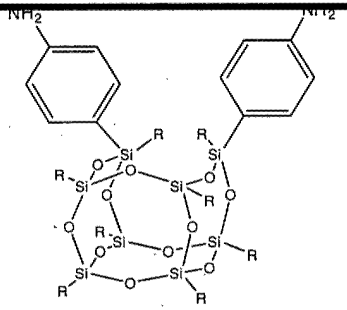

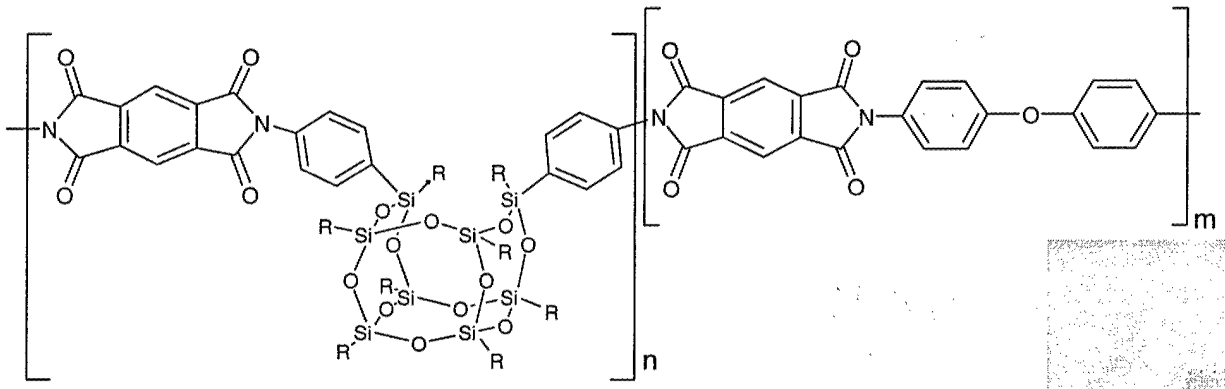

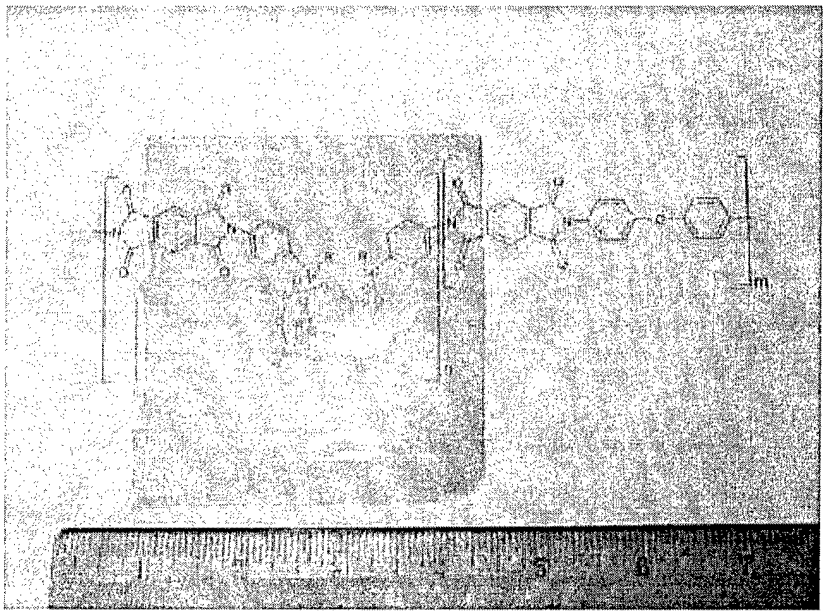

- **transparent films**
- **no aggregates formed**

# POSS High Performance Polyimides

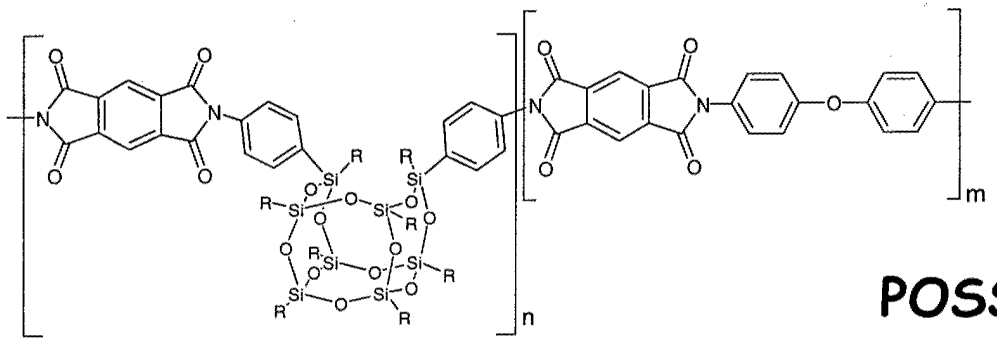

**POSS-Kapton polyimide**

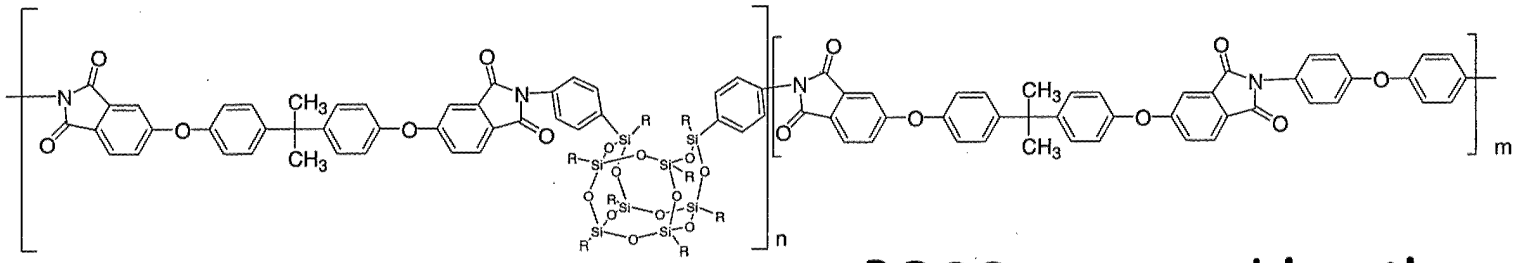

**POSS processable ether-imide**

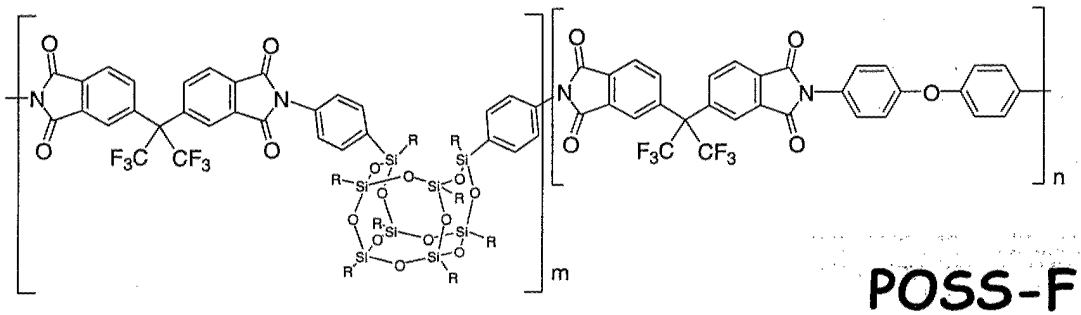

**POSS-Fluorinated colorless polyimide**

UNIVERSITY OF FLORIDA

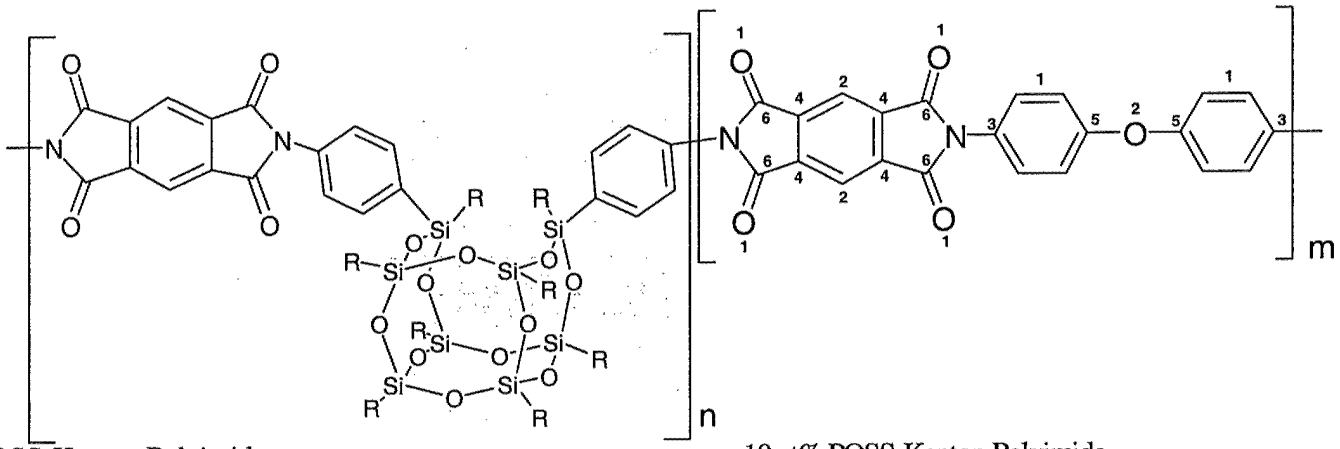

10wt% POSS-Kapton Polyimide

10wt% POSS-Kapton Polyimide

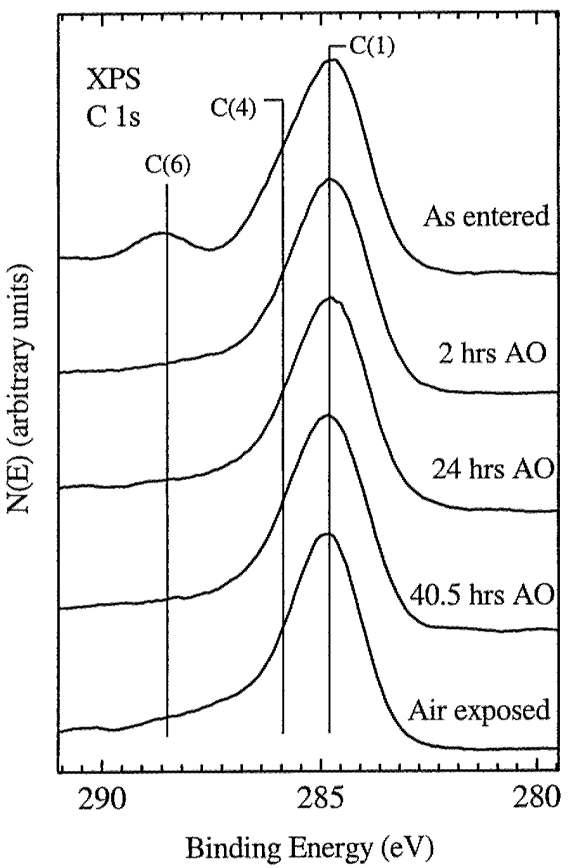


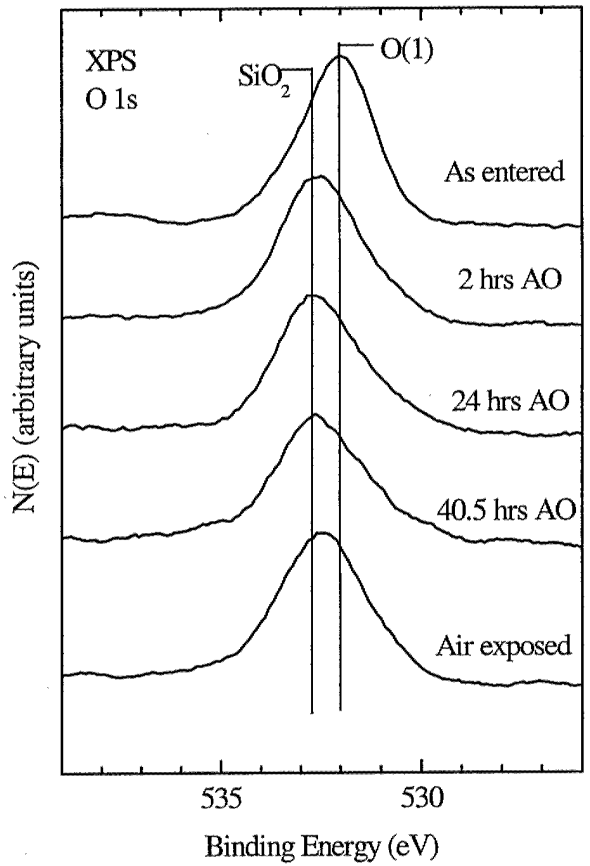

UNIVERSITY OF FLORIDA

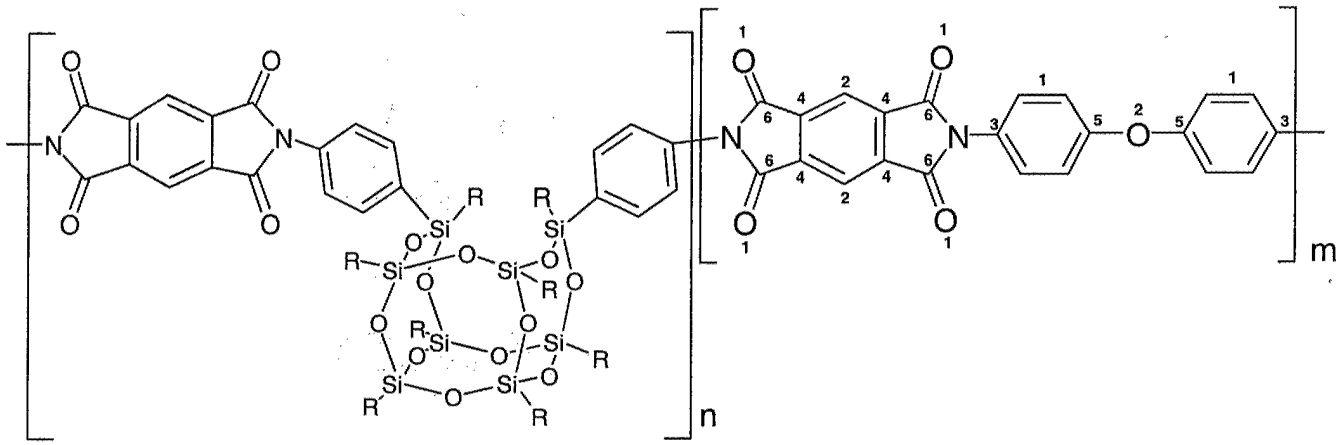

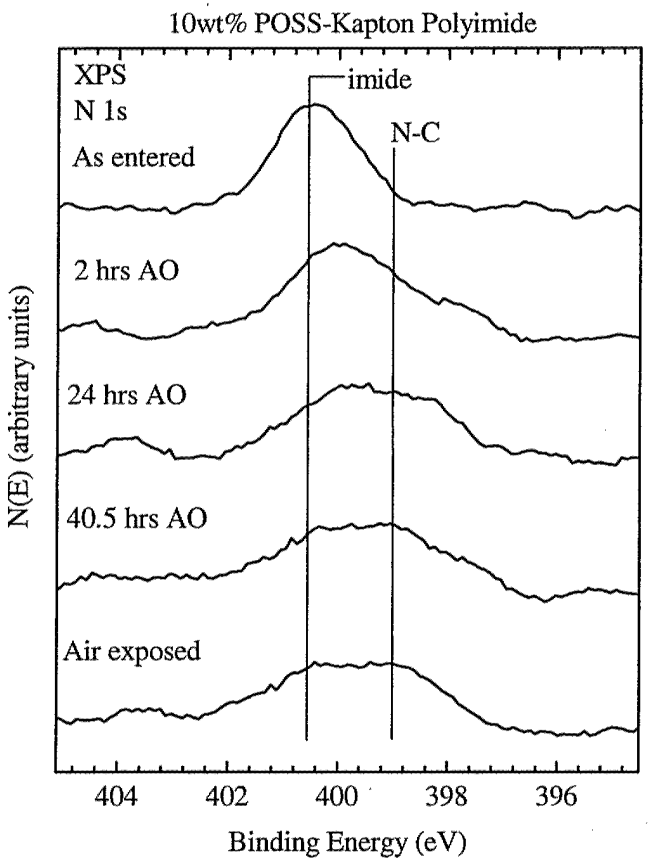


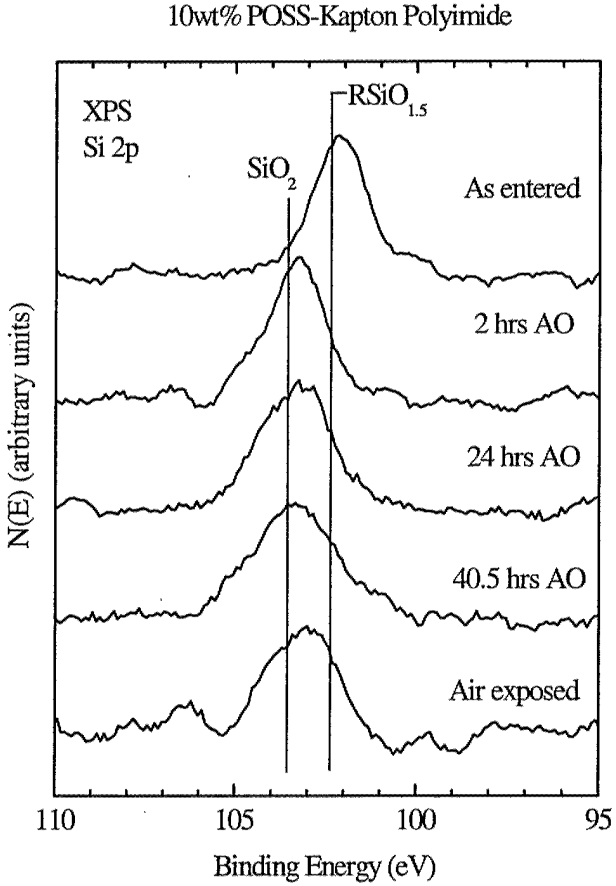

# Beam-Surface Scattering/Atomic Oxygen Test Facility

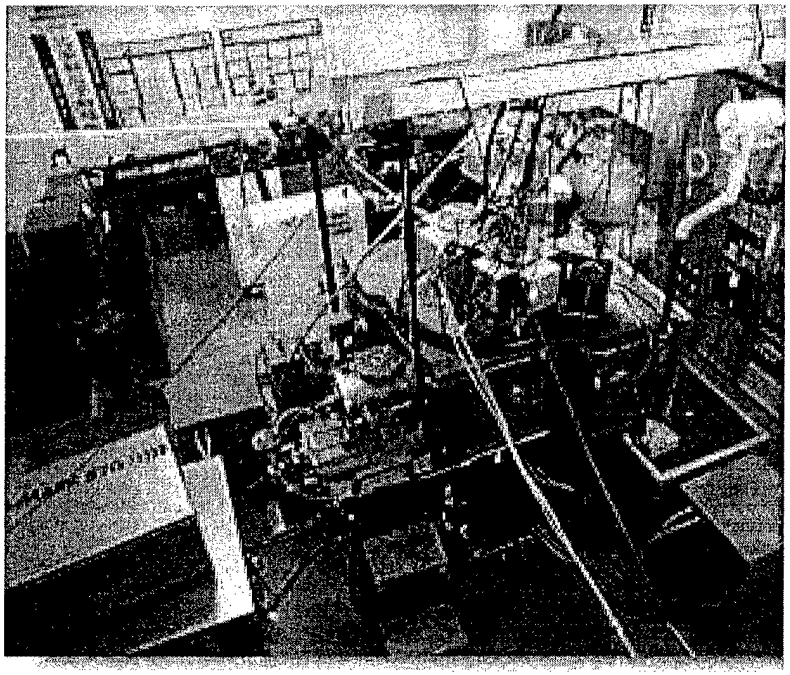

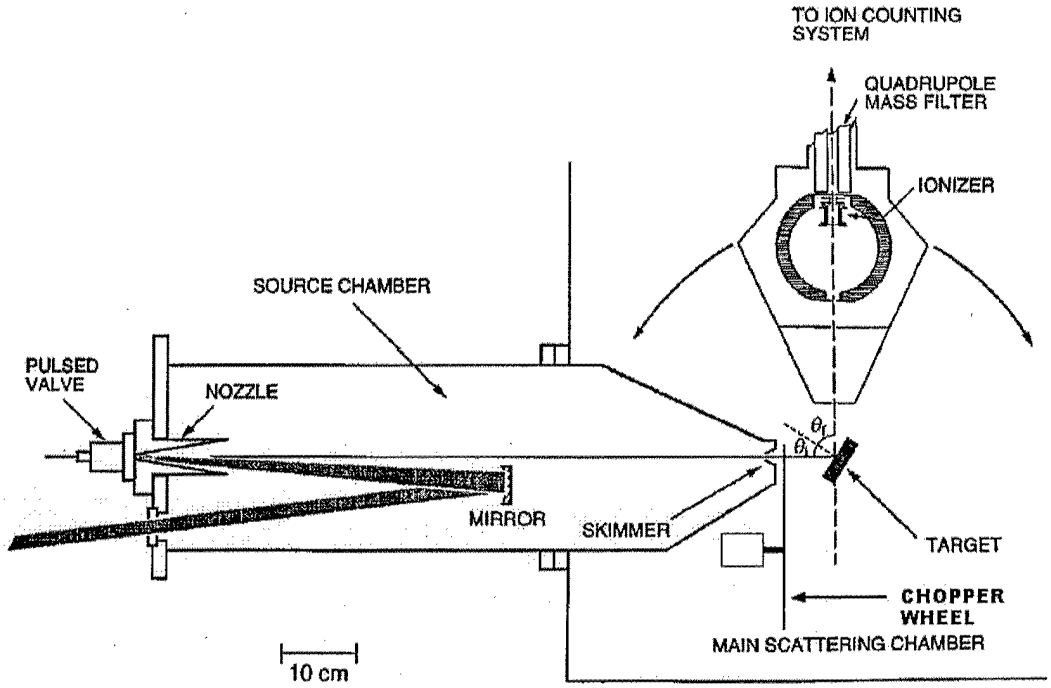


**Pulsed $CO_2$ Laser Atomic Oxygen Generator**

**2-15 eV AO at high fluxes of $10^{16}$ atoms $cm^{-2}$ $sec^{-1}$**

# Surface Topographical Analysis/Profilometry

## Hyperthermal AO Beam

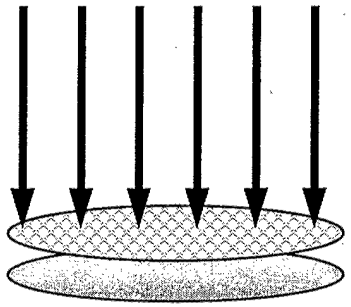

Screen
Sample

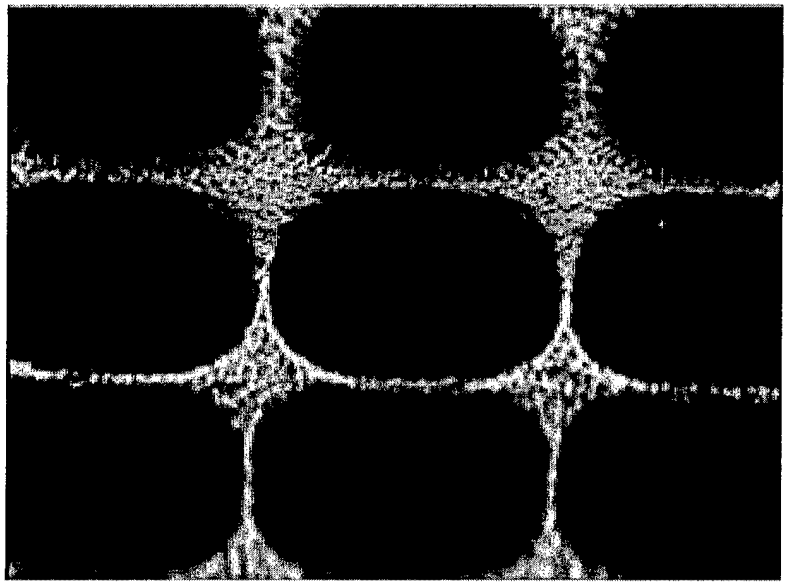

Kapton H

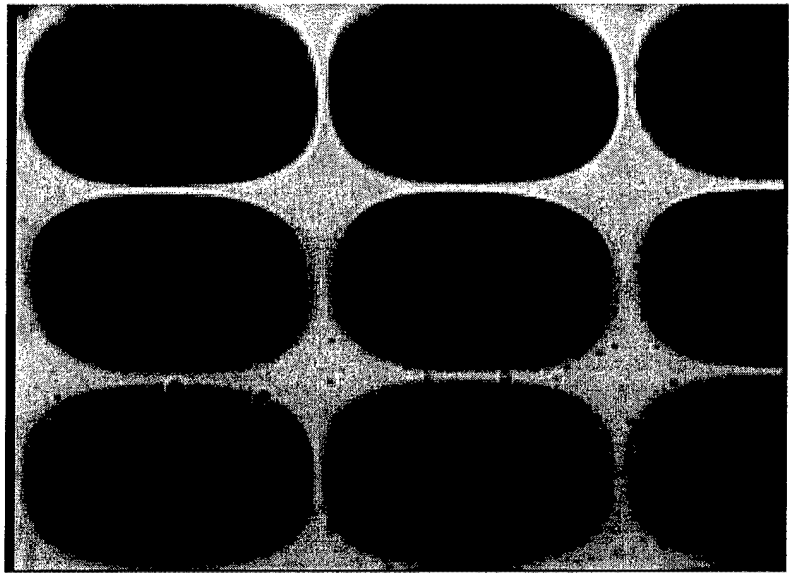

Kapton 10 wt% POSS

# O-Atom etching experiment of POSS-Kapton polyimides
## Total AO fluence of 2.62 x $10^{20}$ atoms/$cm^2$ (~ 3 Days in LEO)

**Hyperthermal AO Beam**

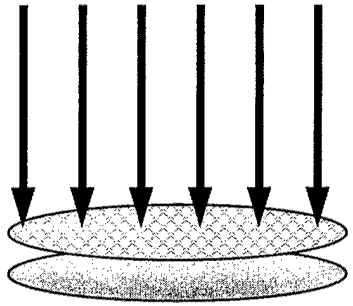

**Screen**
**Sample**

20 wt% POSS in Kapton results in over 20 time improvement in erosion resistance.

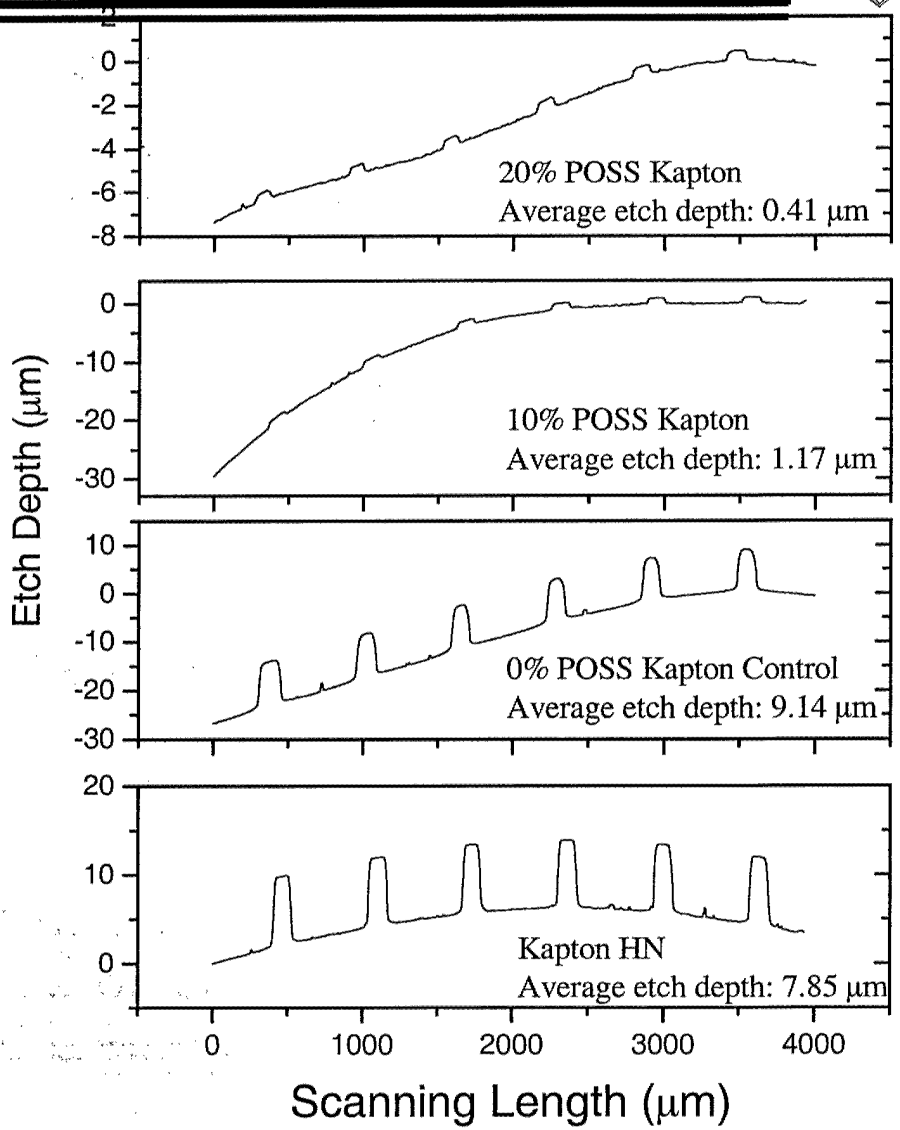

# O-Atom Etching Experiment (~10 DAYS IN LEO)
## Total AO fluence of 8.47 x $10^{20}$ atoms $cm^{-2}$ (100,000 pluses)

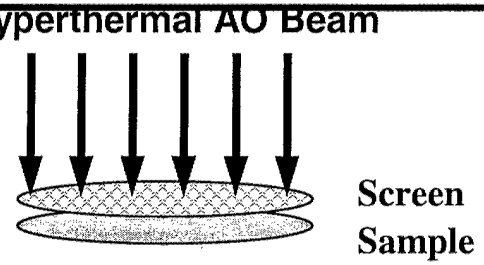


**Kapton 10 wt% POSS**

Average etch depth: **2.2 $\mu$m**

**Kapton H Standard**

Average etch depth: **25.4 $\mu$m**

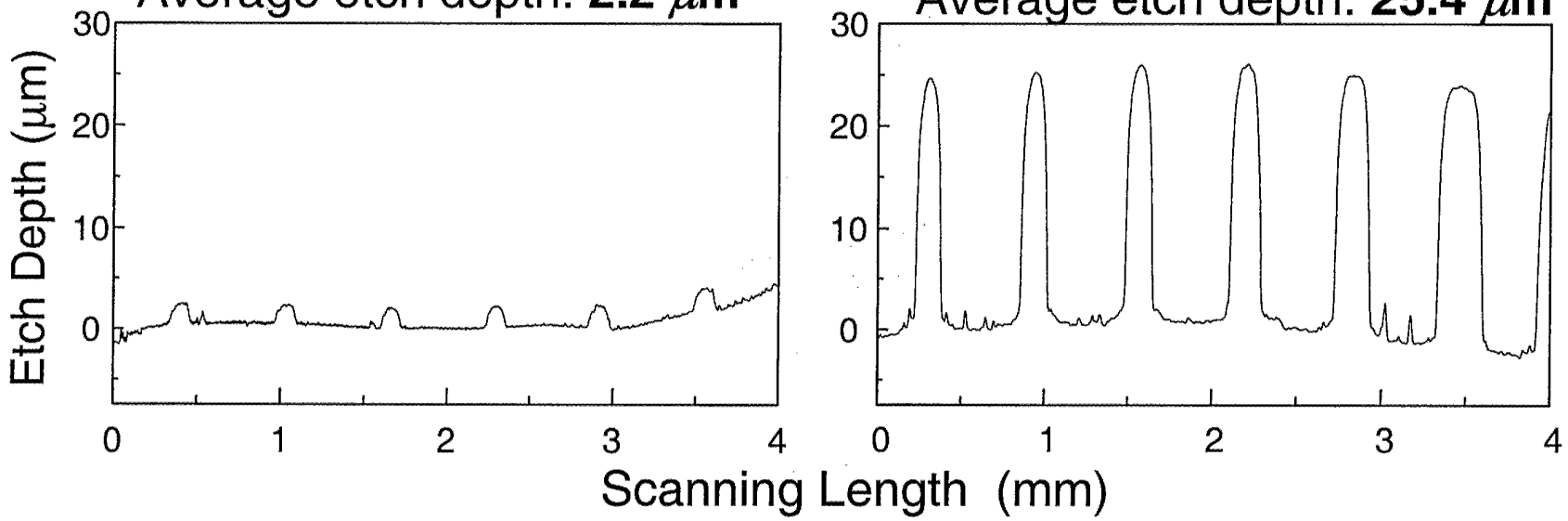


Significantly improved oxidation resistance due to a rapidly formed ceramic-like, passivating and **self-healing** silica layer preventing further degradation of underlying virgin polymer.

# AFM Images of Unexposed POSS Polyimide Films

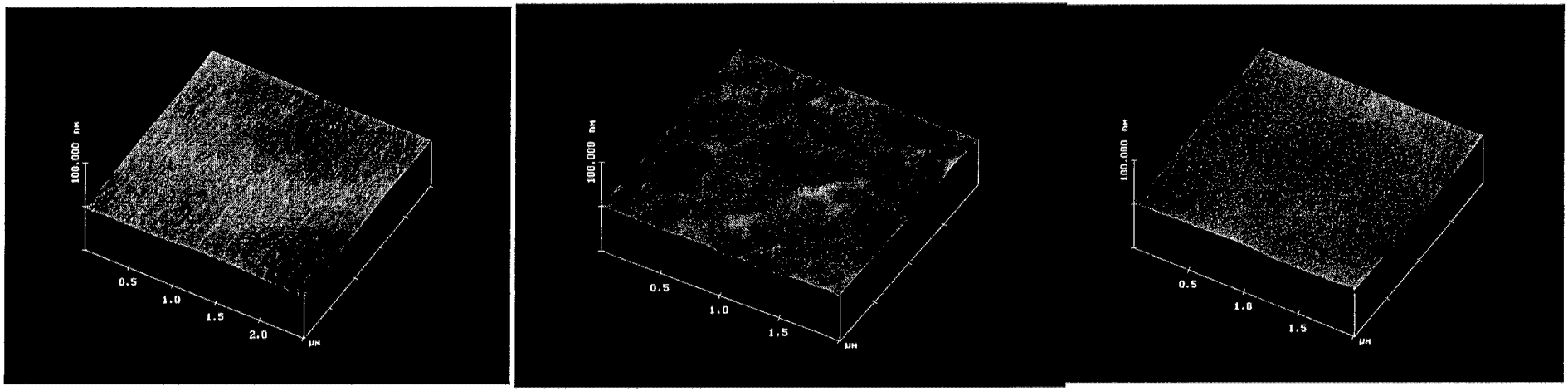


**0% POSS**

**rms roughness: 1.09 nm**

**10% POSS**

**rms roughness: 1.03 nm**

**20% POSS**

**rms roughness: 1.55 nm**

# AFM Images of Exposed POSS Polyimide Films 100,000 Pulses of Hyperthermal (5 eV) AO Beam

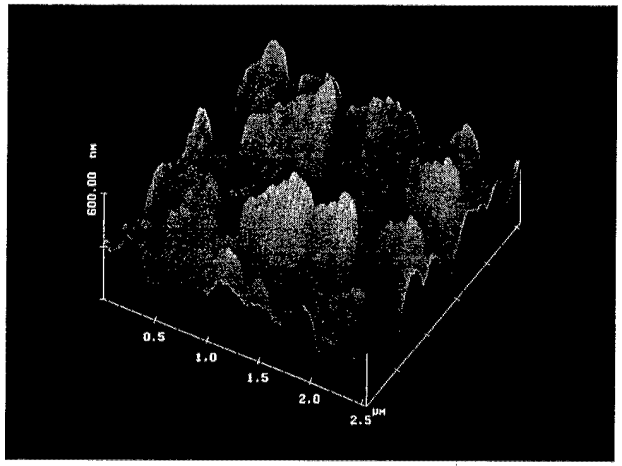


**0% POSS**

**rms roughness: 102 nm**

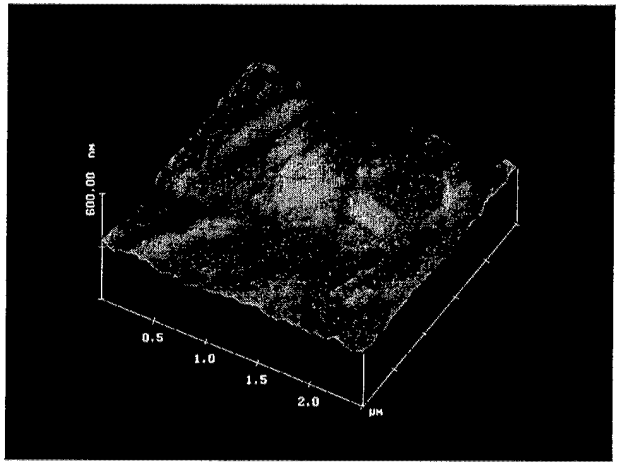


**10% POSS**

**rms roughness: 17.7 nm**

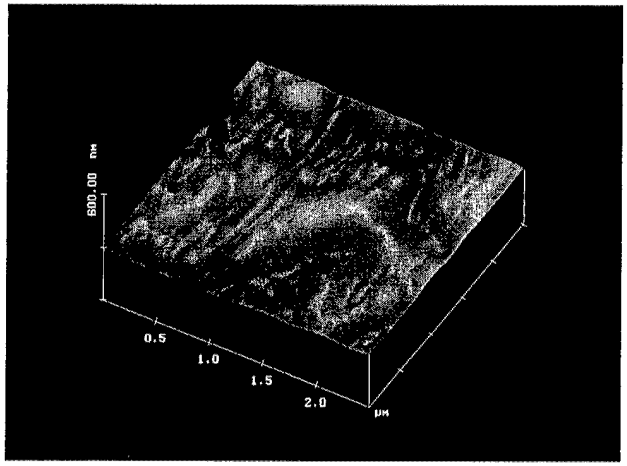


**20% POSS**

**rms roughness: 6.75 nm**

# Erosion of POSS Polyimides by a Beam of Hyperthermal (5eV) O Atoms

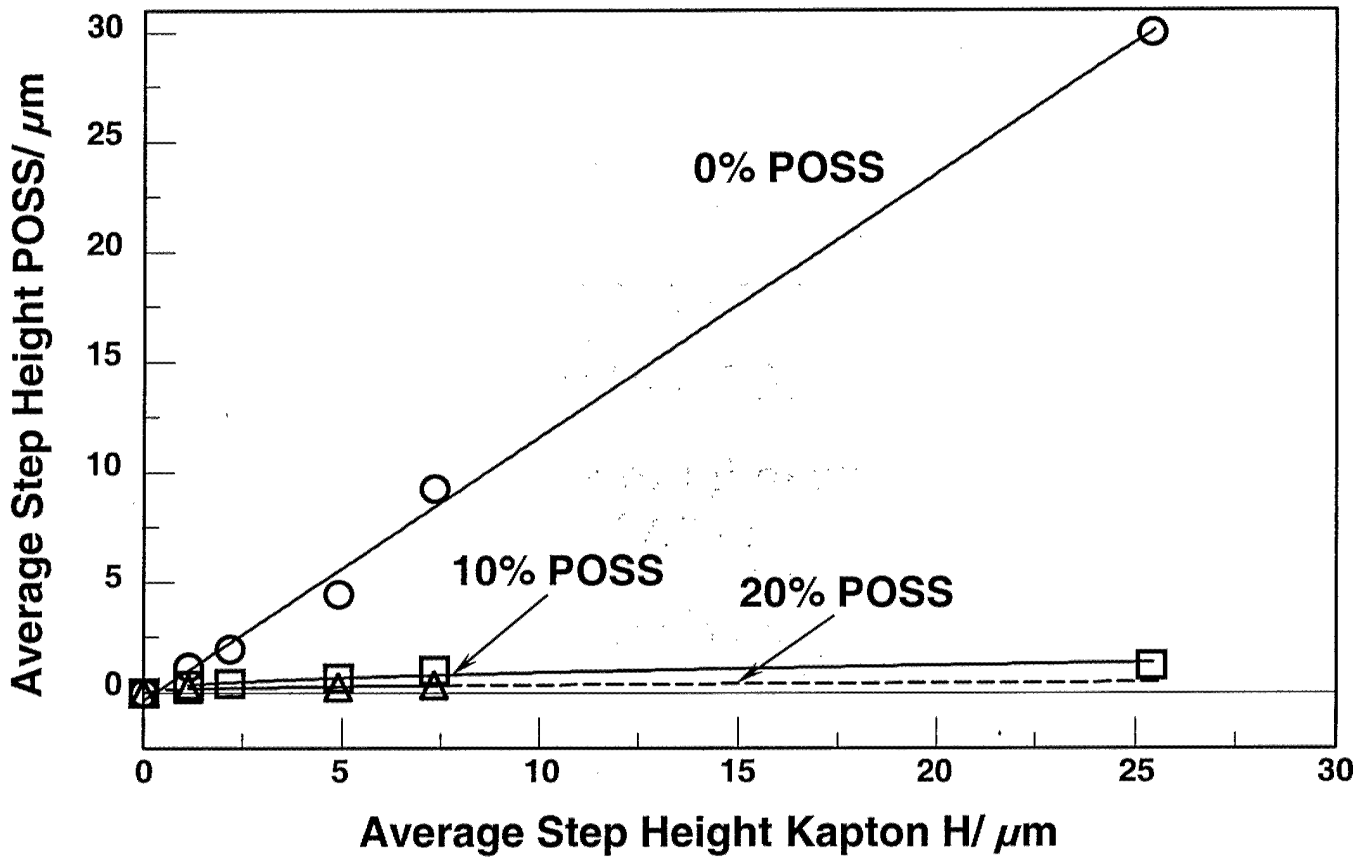


Beam Pulses/ 1000 28 50 100 150 395

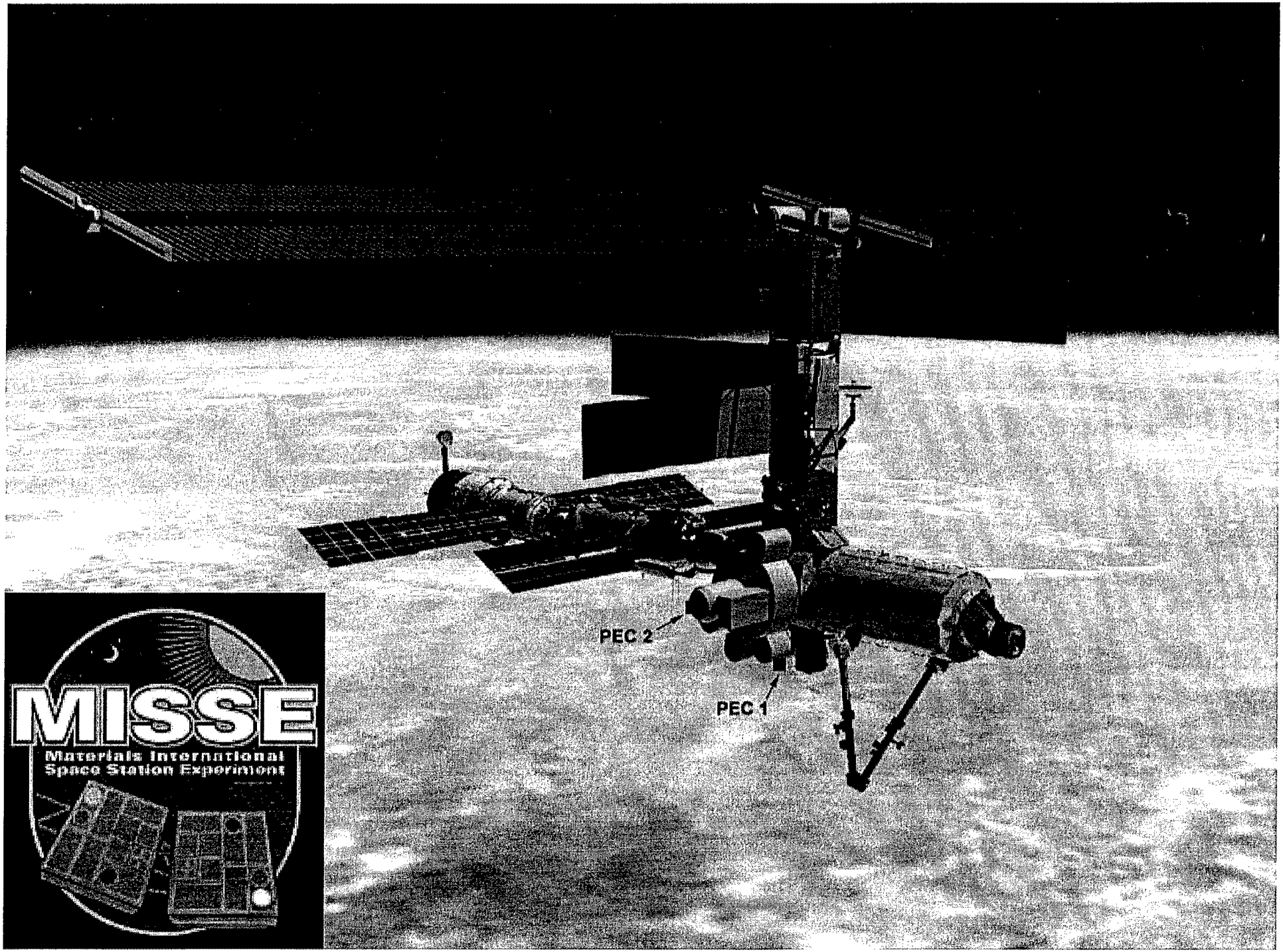
MISSE
Materials International
Space Station Experiment
PEC 2
PEC 1

# MATERIALS INTERNATIONAL SPACE STATION EXPERIMENT

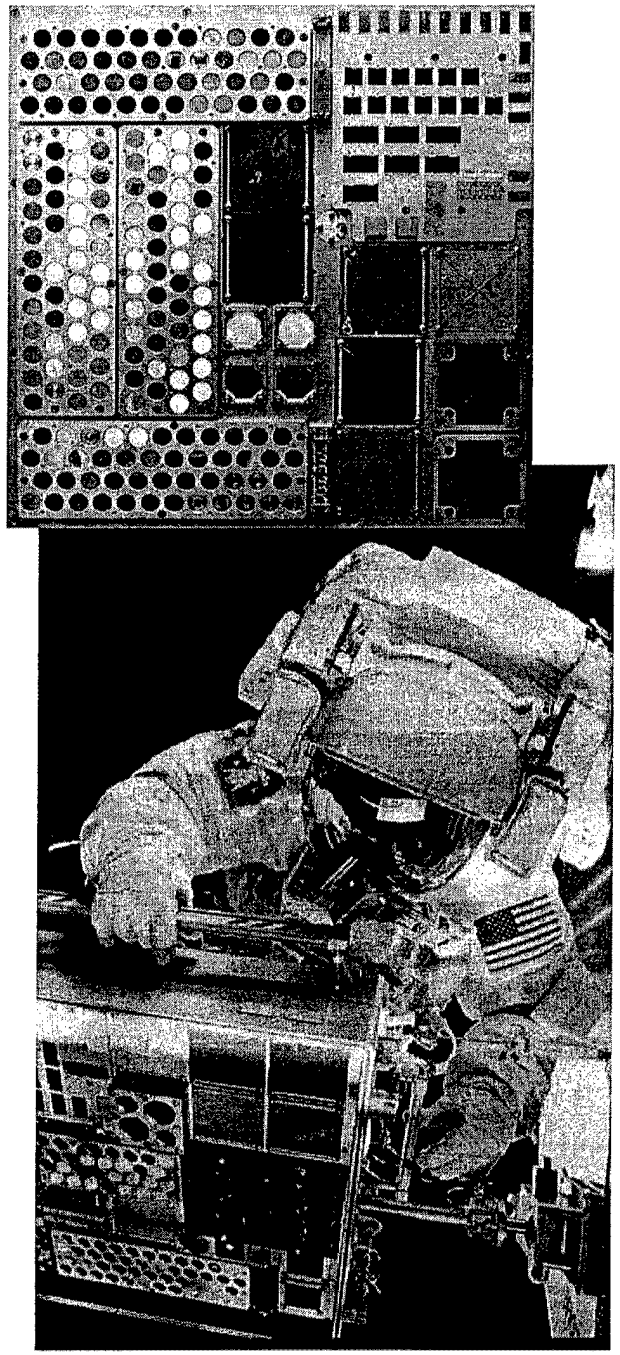

## 18 MONTH EXPOSURE TO LEO

## POSS in Space

## POSS-Polymers Fly on STS 105 Discovery and are deployed on the Int'l Space Station 16 August 2001

**Footage courtesy of NASA**

# Tri-collaborative Effort for Proposed High-Risk, High-Payoff Program (Industry, Academia & Government)

Hybrid Plastics™

POSS-Aniline Synthesis.
Scale up and Validation.

DARPA

UNIVERSITY OF FLORIDA

MONTANA STATE UNIVERSITY BOZEMAN

Space Survivability Testing:
Includes erosion yields, surface Topographical, and in-situ analysis of POSS polymers following atomic oxygen and vacuum ultraviolet radiation exposure .

**Michigan State University**
Thermal, mechanical, and dielectric Properties of POSS-polyimides.

## POSS-Polymeric Materials Group
## Materials Application Branch
## AFRL, Edwards AFB

Efficient cost effective POSS-Aniline Monomer and POSS-Polyimide Synthesis.
Development, characterization, and testing of POSS-Polyimide composite materials with high temperature stability and space survivability.

tsi TRITON SYSTEMS INC

POSS Incorporation in Triton's High Performance Polyimide Resins:
Triton RTM PMR polyimides and NASA and Triton's co-developed Phosphine Oxide Polyimides.
Scale up and Validation.

THE AEROSPACE CORPORATION

Space Survivability Testing:
Includes simulated GEO exposure and mechanical property testing prior to and following exposure.

# AFM Images of Unexposed Polyimides Copolymerized With Various Weight Percents of POSS

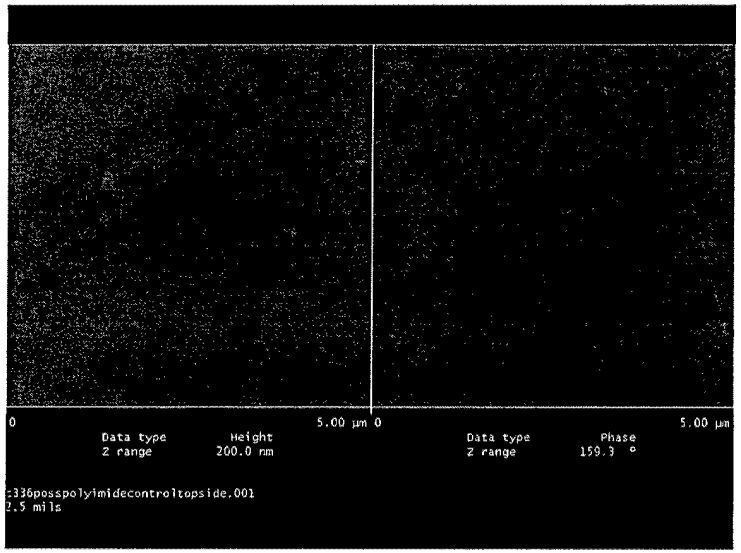


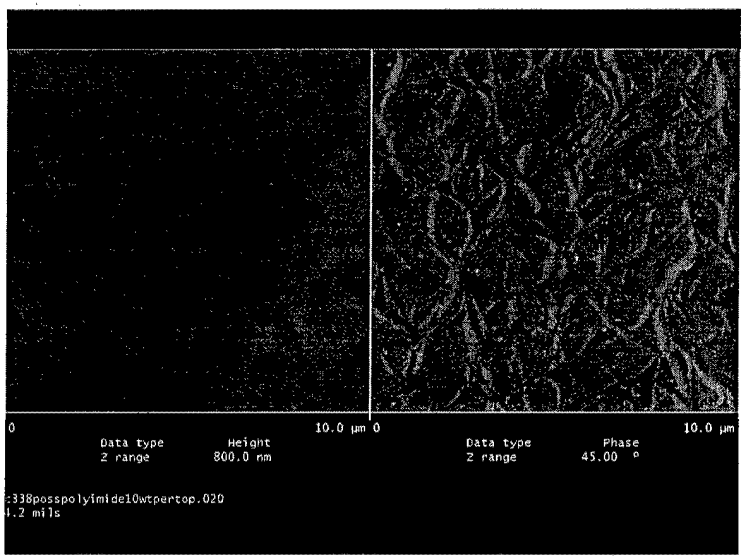


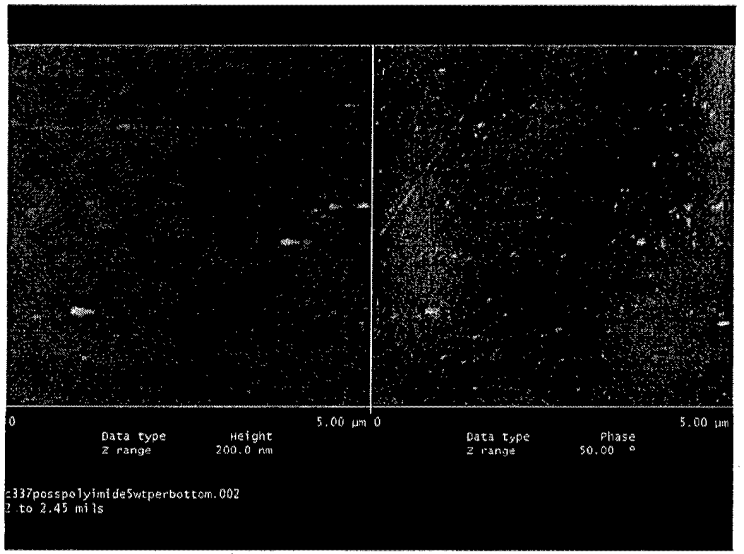


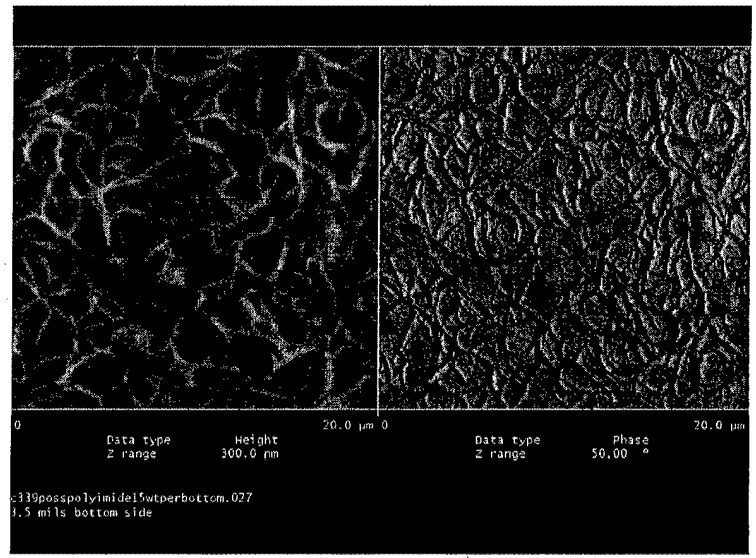

# Three dimensional AFM Images 10 wt % POSS Polyimide Films

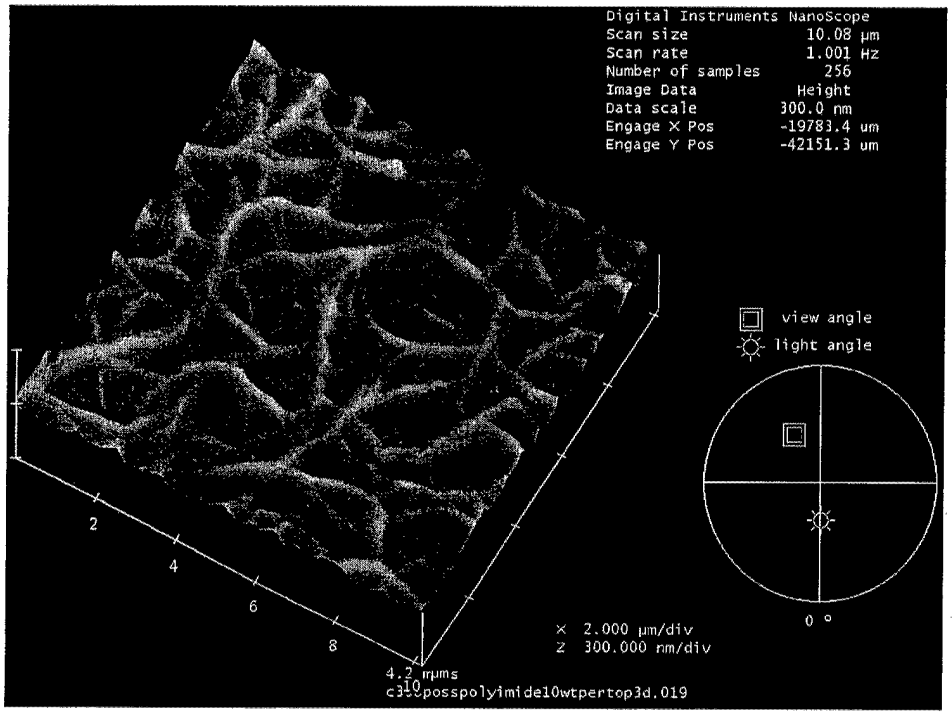


**Unexposed**

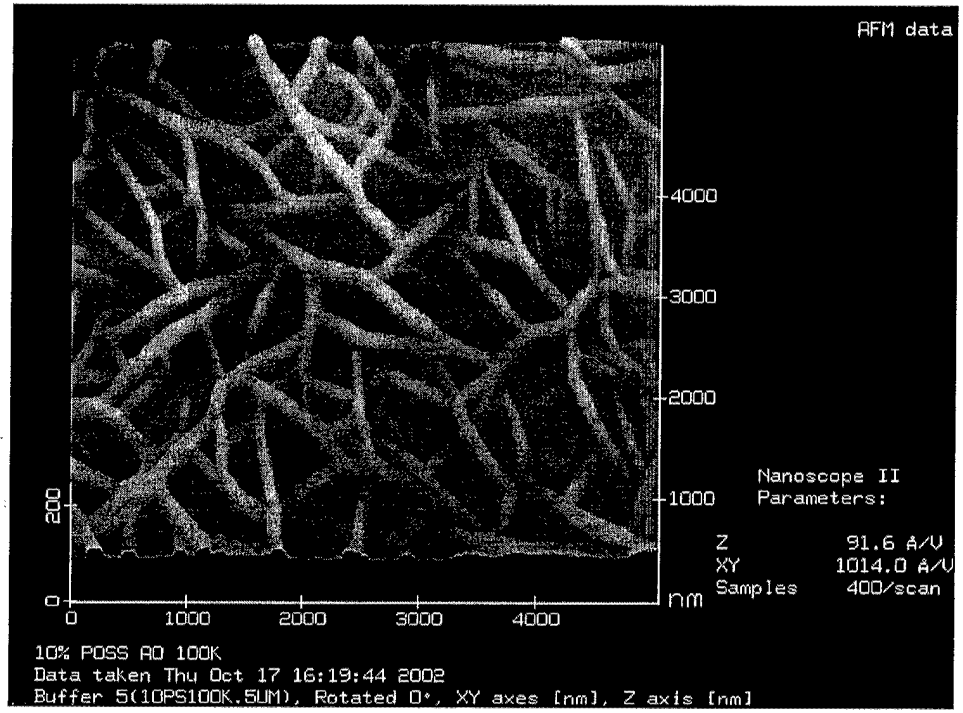


**Exposed**

# Polyimides in Propulsion

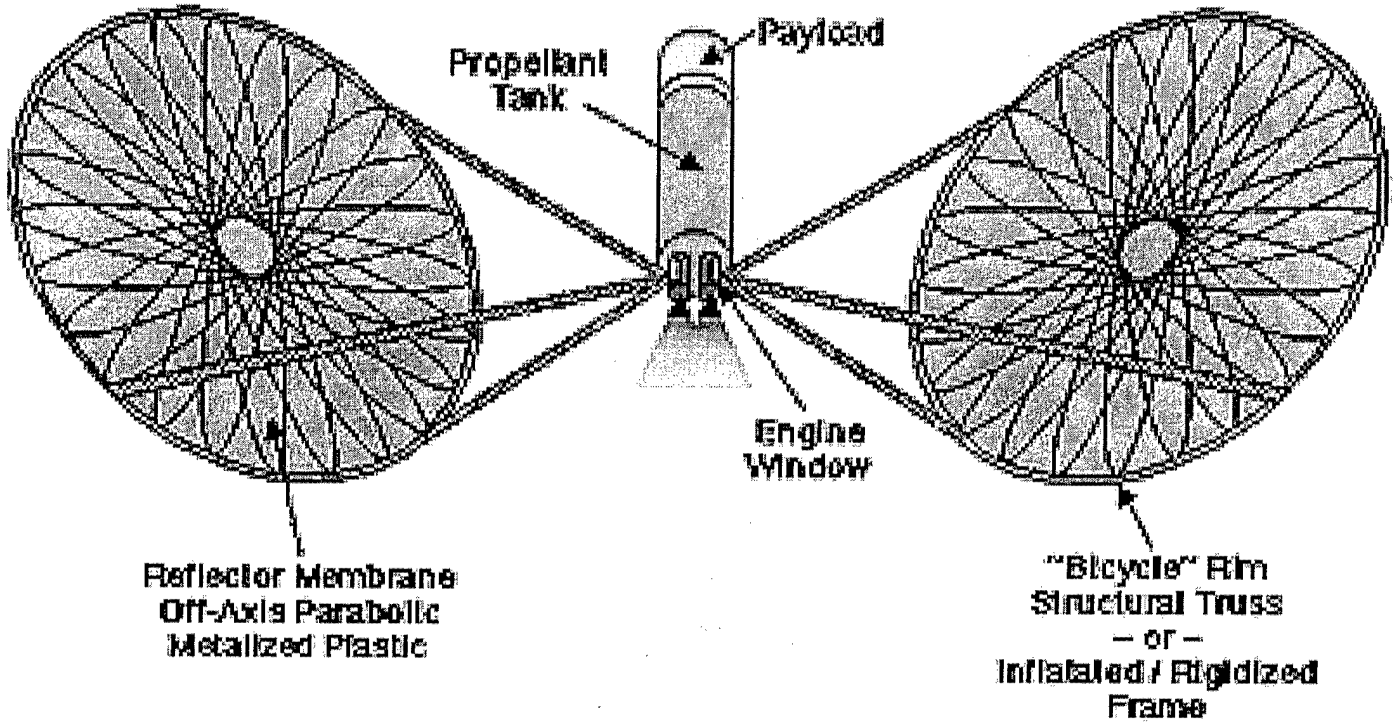


In a solar/laser thermal rocket, solar or laser light is collected and focused to heat a propellant working fluid such as hydrogen. **The collector mirrors are silvered balloon-like Inflatable structures or thin sheets of silvered plastic supported by lightweight inflatable trusses.** The light passes through a high temperature quartz window or into an open cavity on the side of the engine and focuses to a point to either directly heat the hydrogen propellant or heat a material such as graphite which then heats the hydrogen propellant.(Air force Phillips Laboratory and the NASA Marshall Spaceflight Center.)

# Polyimides in Propulsion

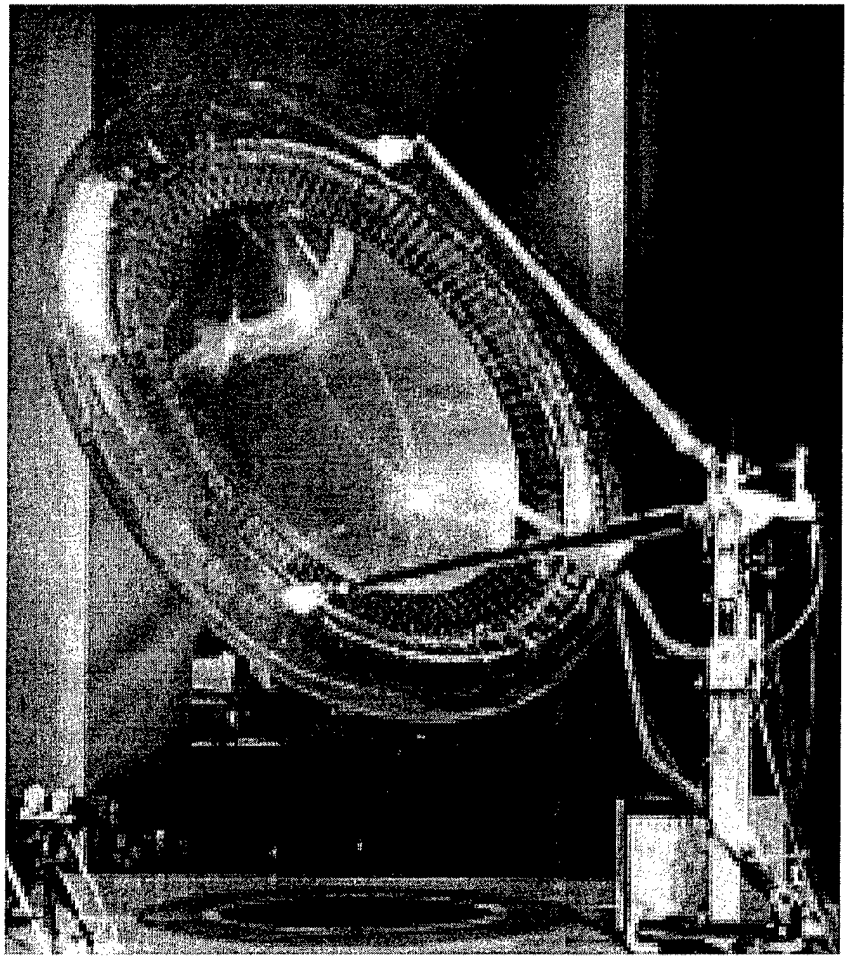

*SRS Technologies'* (Huntsville, Alabama), ***solar concentrators are made almost entirely of castable, clear polyimide film****, a lightweight material compared to glass or metal optics.*